# CHARACTERIZATION OF SOLID ACID CATALYSTS

# FOR ISOBUTANE/BUTENE ALKYLATION

By

ALEXANDRU PLATON

A dissertation submitted in partial fulfillment of
The requirements for the degree of

DOCTOR OF PHYLOSOPHY

WASHINGTON STATE UNIVERSITY
Department of Chemical Engineering

DECEMBER 2004

To the Faculty of Washington State University:

The members of the Committee appointed to examine the dissertation of ALEXANDRU PLATON find it satisfactory and recommend that it be accepted.

_____
Chair

_____

_____

_____

ACKNOWLEDGEMENTS

I would like to thank Dr. William J. Thomson for his invaluable advice and help with defining my research goals and building the necessary self-confidence in order to finalize this work. I would also like to express my thanks to my committee members, Dr. Kerry W. Hipps, Dr. Reid C. Miller and Dr. Richard L. Zollars, for their inexhaustible patience towards my many hesitations along this work. Many thanks go to my close friends and fellow researchers Sekar Darujati, Dr. David C. Lamont and Dr. Rakesh Radhakrishnan for being very patient listeners and for providing excellent technical advice, as well as to Diana Thornton, Jo Ann McCabe and Paul Golter for their help with technical and administrative issues.

Most of this work was carried on in, and funded through, the O.H. Reaugh Laboratory for Oil and Gas Processing Research.

CHARACTERIZATION OF SOLID ACID CATALYSTS

FOR ISOBUTANE/BUTENE ALKYLATION

Abstract

By Alexandru Platon, Ph.D.
Washington State University
December 2004

Chair: William J. Thomson

The extinction coefficient ratio (ECR) of coordinatively bonded pyridine (Lpy) and protonated pyridine (Bpy) was determined by diffuse-reflectance FTIR spectroscopy (DRIFTS), by exposing sulfated zirconia (SZ) containing chemisorbed pyridine to water vapor. The previously suggested portability of published ECR values between different IR spectroscopy techniques or different types of materials was found questionable. For the SZ samples analyzed, an ECR value of 2.05 was determined, which allowed the measurement of an initial Lewis/Brönsted acidity ratio of 1.1 in the freshly activated material. This ECR determination method should be applicable to other similar solid acids.

In a separate study, a new model test reaction was proposed for the estimation of low-temperature hydride transfer (HT) activity of solid acids. The reaction of cyclohexene with isobutane on zeolites Beta having $SiO_2/Al_2O_3$ ratios of 25 (25BEA) and 75 (75BEA), ZSM-5 and SZ, distinguished between disproportionation/hydrogen transfer (DHGT) and HT. HT was enhanced in 25BEA due to its higher acid density. On the other hand, the very high acid density SZ was less active than expected for HT due to its low isobutane adsorption capacity. ZSM-5 completely lacked HT activity although it showed significant DHGT activity.

Finally, the catalytic behavior of the mentioned catalysts was studied in gas-phase, batch alkylation experiments employing isobutane and 1-butene at 80 °C. The observed alkylation

performance was compared to their low-temperature HT activity, total acidity, adsorption capacity and surface area. The measured HT activity correlated with the amount of trimethylpentane produced per acid site for all materials with 25BEA being the most active and ZSM-5 being totally inactive for alkylation. Although of moderate alkylation activity, SZ had a higher cracking activity than other materials. Modification by water vapor exposure of 25BEA and SZ did not noticeably change their Brönsted acidity, but selectively lowered their alkylation activity by competitive adsorption between water and isobutane. The apparent butene conversion correlated well with the total catalyst surface area rather than with the total amount of acid sites. Evidence indicates that competitive adsorption with butene limits isobutane access to the active sites in all studied materials, resulting in limited hydride transfer.

TABLE OF CONTENTS

## Dedication

This work is dedicated to my wife, Codruta, and my son, Alex Jr., who supported me through the last five years with their limitless confidence and encouragement.

# CHAPTER ONE

# GENERAL INTRODUCTION

This work consists of three manuscripts, included in Chapters 2, 3 and 4, which follow the formats required by the journals Industrial and Engineering Chemistry Research, Catalysis Letters and Applied Catalysis A: General, respectively. Additionally, a general introduction and supporting appendices are included in the standard dissertation format. The manuscripts are coauthored with Professor W.J. Thomson. Mr. Platon contributed with the experimental work, data analysis and manuscript writing, while Professor Thomson contributed with guidance, knowledge and organization of manuscript ideas.

## Background on Alkylation

From the total US gasoline pool, alkylate constitutes the component having the third most important contribution to the octane number (Table 1.1 [1]), being surpassed only by reformate (composed mostly of aromatic hydrocarbons and isoparaffins) and catalytic cracker gasoline (composed mostly of olefins). Several drawbacks are associated with both reformate and the cat cracker gasoline. Aromatic hydrocarbons are carcinogens and environmental hazards, especially if they contaminate aquifers adjacent to gasoline storage and distribution facilities. Olefins on the other hand have an elevated tendency to polymerize in the presence of ambient oxygen with the subsequent formation of polymeric deposits in tanks, ducts and fuel injectors; in the quest to increase the fuel efficiency of the internal combustion engine, restrictions in the allowed content of polymer precursors are expected to affect the allowed proportion of cat cracker gasoline in the total pool. Besides alkylate, other high octane number components that could constitute alternatives include the butane fraction, characterized however by a high volatility and only suitable for cold climates, and oxygenate components, which have a lower heat of combustion

than hydrocarbons and are either toxic (methanol), expensive or dangerous to the environment (ethers easily contaminate aquifers). Alkylate constitutes a very promising alternative to all the above-mentioned components as it is non-reactive, nontoxic and has a low volatility.

The refinery process of isobutane alkylation with olefins, although a commercial success, is based on liquid acid catalysts such as hydrofluoric acid and sulfuric acid, which are very corrosive, and either relatively expensive to recover ($H_2SO_4$), or very dangerous in case of an accidental release (HF). The process is making use of refrigeration in order to achieve the required low reaction temperatures (typically 5–15 °C). Comparatively, a solid acid catalyst would be more convenient in terms of reaction temperature, safety and recovery. Researchers from the SunOil laboratories observed in pioneering studies that an exchanged zeolite was active for alkylation catalysis at temperatures between 25–100 °C [2]. A major drawback, however, evidenced in all laboratory-scale evaluations of solid acid catalysts for alkylation is their rapid deactivation.

Despite the fact that other successful refinery processes in which the catalyst deactivates within fractions of a second have been used for decades (FCC, or fluid catalytic cracking), current constraints in a refiner's economics arising from such factors as oil price fluidity and emerging environmental policies are making investments in new processes unattractive. Moreover, the current material balance of the typical US refinery is making use of most of the $C_3$-$C_4$ fraction available [1]. Refiners will most probably lack motivation to adopt a new solid-acid-based alkylation process unless particularly stable catalysts and promising technologies are identified.

**Alkylation on solid acid catalysts**

The global reaction and principal mechanism for isobutane alkylation with butene are depicted in Figure 1.1. The relative rates of the elementary processes involved determine the outcome of the overall alkylation process, with the most important products being the $C_8$ isoalkanes. Most notable is the step involving the octyl carbenium ion that is usually accompanied by side reactions characteristic of the carbocation chemistry. These side reactions include isomerization, multiple olefin addition, cracking and dehydrogenation, some of which are thought to be responsible for catalyst deactivation. One major factor determining these side processes is the $C_8$ intermediate lifetime, which in turn is determined by the rate of hydride transfer from isobutane. It is therefore the relative rate of hydride transfer that seems to play an important role in the alkylation process.

A recurring finding from studies on solid acid-catalyzed alkylation is that the catalyst deactivates after a very limited number of alkylation turnovers due to loss of hydride transfer activity. Indications were found that the type, strength and density of acid sites are factors that determine catalyst performance during alkylation. The initial subject of research in this work was the identification of key catalyst characteristics that would lead to a successful solid-acid catalyst for the alkylation of isobutane with 1-butene. The emphasis on catalyst characterization led to efforts to develop novel methods of quantifying Lewis and Brönsted acidity on solid acids and of measuring the "true", Rideal-type bimolecular hydride transfer between isobutane and larger hydrocarbon intermediates. Finally, these characterization techniques, complemented by total acidity and reactant adsorption measurements, were employed in a comparative study of the catalytic behavior of several solid acids in batch, gas-phase alkylation tests.

**Solid acid catalyst characterization**

The solid acid catalysts chosen in this study are Beta (BEA) zeolite and sulfated zirconia (SZ), both of which were previously found to have some activity in the alkylation reaction, as well as ZSM-5, which is a known cracking catalyst previously evidenced to lack alkylation activity. Comparing several types of solid acids allowed to evaluate the effect of the catalytic material type on alkylation. An important characteristic of silica-alumina zeolitic acids is their $SiO_2/Al_2O_3$ ratio (SAR), which determines the theoretical density of acid sites. Two SAR values were chosen for the BEA material: 25 (high acid density) and 75 (low acid density). This way, the effect of acid density upon alkylation activity could be evaluated. The four mentioned catalysts were characterized for their acidity type (Lewis/Brönsted), total acidity, as well as their interaction strength with the reactants isobutane and 1-butene. A short introduction to each characterization method is given below, along with pointers to the material in the following chapters and appendices.

*Lewis/Brönsted DRIFTS*

Some controversy exists regarding the nature of acid sites responsible for sustained hydride transfer activity and, hence, prolonged alkylation activity. [3,4] An attempt was initially made to measure the relative concentrations of Lewis and Brönsted acidity on the mentioned catalysts and then estimate their effect on alkylation activity. A diffuse-reflectance FTIR spectrometer (DRIFTS) setup was employed in this respect, based on the fact that pyridine interacting with Lewis (Lpy) and Brönsted (Bpy) acids has different infrared spectra. While no success was recorded in detecting any Brönsted acidity in the freshly activated zeolites 25BEA and 75BEA (activation details are given in Chapters 3 and 4), in the case of SZ both acid site types were detected. However, as emphasized in Chapter 2, in an attempt to quantify the Lpy/Bpy concentration ratio in SZ, no reliable source for the otherwise assumed-constant extinction

coefficients could be identified. Noting reports that Lewis and Brönsted sites readily interchanged in SZ under the effect of water exchange, the setup in Figure 1.2 was used to simultaneously measure the extinction coefficient ratio and concentration ratio for the Lpy and Bpy species in SZ, as shown in Chapter 2. Further details regarding the statistical data processing involved are also given in Appendix A.

*Adsorption measurements: ammonia chemisorption and isobutane adsorption capacity*

Knowledge of the number of active sites is essential when different materials, or materials with different active site densities are compared. Catalytic reaction rates expressed in terms of per-site turnovers per unit time are a direct indication of the catalytic activity when all other reaction conditions are held constant. Titration with a base such as ammonia is a convenient method to measure the number of acid sites in solids, and temperature-programmed desorption and the volumetric measurement of chemisorption isotherms are among the most frequently used titration techniques. In this study volumetric measurements of ammonia chemisorption isotherms were used to determine the total acidity of the studied catalysts. An ASDI RXM-100 catalyst characterization apparatus capable of a theoretical sensitivity of ~ $5x10^{-6}$ mmol was used for this purpose.

Crucial for the accuracy of these measurements is the knowledge of the dry weight of the catalyst samples investigated. Moreover, as shown in Chapters 3 and 4, some of the catalysts studied were obtained in their ammonium-exchanged form, and required a decomposition step in which acid sites are released from the interaction with ammonia. Samples from each catalyst were subjected to thermogravimetric/mass spectrometry (TG/MS) studies that allowed the simultaneous measurement of the dry mass as well as the optimal decomposition/dehydration (activation) temperatures.

Details regarding the TG/MS measurements and data acquired are given in Chapters 3, 4, as well as in Appendix B. The experimental procedure and calculation method involved in the volumetric acid site titration with ammonia are described in Appendix B and the experimental data acquired is also included. Attempts were also made to quantify the chemisorption of alkylation reactants – isobutane and 1-butene. However only the amount of physisorbed isobutane could be measured on the above-mentioned catalysts, as shown in Chapters 3, 4, and Appendix B.

*Hydride transfer activity characterization*

Since hydride transfer (HT) seems to be an important factor in alkylation as emphasized above, a method was sought to directly measure the HT activity of the studied catalysts at a temperature that is relevant to the alkylation reaction, differentiating at the same time between the "true", Rideal-type hydride transfer and hydrogen transfer from carbonaceous deposit on the catalyst. Based on observations that cyclohexene was reluctant to cracking at relatively elevated temperatures, a new test method for the measurement of low temperature HT activities was devised. Tests on all catalysts in an experimental setup similar to that in Figure 1.3 showed that the reaction between cyclohexene and isobutane only yielded products of HT and isomerization at 80 °C. Moreover, the particular chemistry of the reaction system chosen allowed for the active sites involved in HT processes to be titrated, as shown in Chapter 3. The raw experimental data is included in Appendix D.

*Alkylation reaction tests*

In order to evaluate the effect of the measured catalyst characteristics on alkylation activity, a simple batch reactor setup was used (Figure 1.4) in which catalysts were contacted with a constant feed mixture based on a constant butene/acid site ratio. As shown in Chapter 4, the four catalysts were compared in terms of 2,2,4-trimethylpentane, dimethylhexanes, $C_8$ olefin and n-pentane productivities per active site. The effect of water vapor pre-exposure for 25BEA

and SZ was also tested, although no change in the relative Lewis/Brönsted population could be induced. The raw numerical results from the alkylation reaction tests are included in Appendix E.

*References*


1. K.D. Miller, Jr., DeWitt & Company Inc., *Alkylates. Key components in clean-burning gasoline,* presented to the Clean Air Act Advisory Committee Panel on Oxygenate Use in Gasoline, May 24, 1999 (www.epa.gov/otaq/consumer/fuels/oxypanel/dxmiller.ppt, accessed 9/13/2004).
2. F W. Kirsch, J.D. Potts, D.S. Barmby, Proceedings - American Petroleum Institute, Division of Refining 48 (1968) 1000.
3. A. Feller, I. Zuazo, A. Guzman, J.O. Barth, J.A. Lercher, J. Catal. 216 (2003) 313.
4. L. Fan, I. Nakamura, S. Ishida, K. Fujimoto, Ind. & Eng. Chem. Res. 36 (1997) 1458.

Table 1.1. Octane number (O.N.) contributions from components of a typical US gasoline. [1]

(MTBE – methyl-*tert*-butylether; TAME – *tert*-amyl-methylether)

| Gasoline Component | % of Pool | Blending O.N. | Contribution |
|---|---|---|---|
| Reformate | 41.40 | 88 | 36.4 |
| Fluid cat cracker gasoline | 26.40 | 86 | 22.7 |
| Alkylate | 14.30 | 93 | 13.3 |
| Isomerate | 7.40 | 87 | 6.4 |
| Alcohols | 3.40 | 108 | 3.7 |
| Light straight-run gasoline | 1.90 | 73 | 1.4 |
| Hydrocracker gasoline | 1.60 | 81 | 1.3 |
| MTBE | 1.00 | 110 | 1.1 |
| n-Butane | 1.10 | 92 | 1.0 |
| Light delayed cocker gasoline | 1.20 | 78 | 0.9 |
| TAME | 0.30 | 105 | 0.3 |
| Total | 100.00 | | 88.6 |

$$iC_4H_{10} + C_4H_8 \rightarrow iC_8H_{18}$$

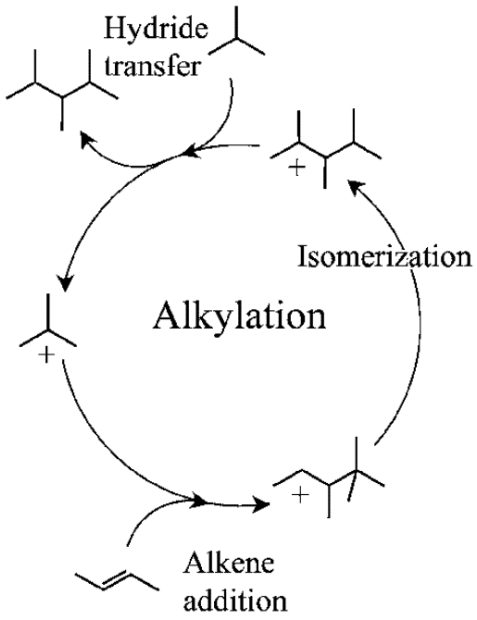


Figure 1.1. Global reaction and main elementary steps in the alkylation of isobutane with butene.

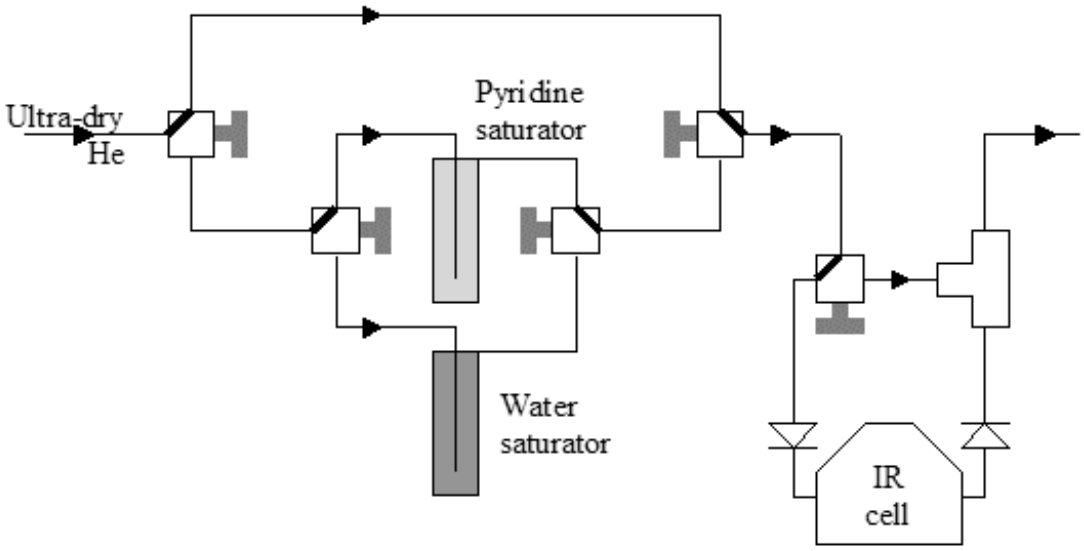


Figure 1.2. Experimental setup for the simultaneous measurement of the Lewis/Brönsted extinction coefficient ratio and concentration ratio.

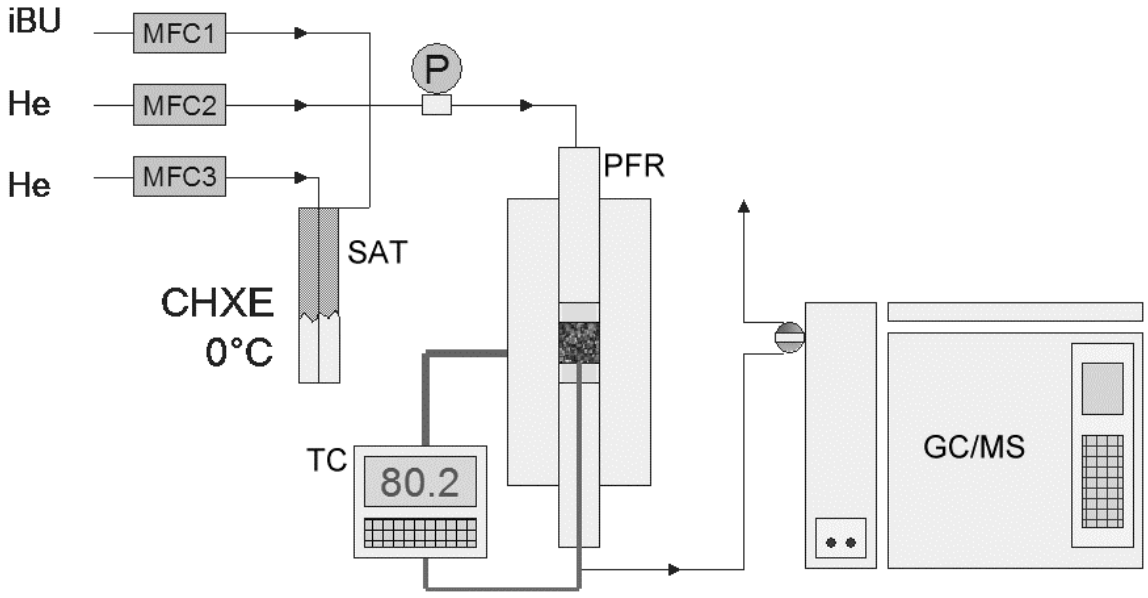


Figure 1.3. Experimental plug-flow reactor setup for the measurement of hydride transfer activities. (PFR – plug-flow reactor setup; SAT – saturator; GC/MS – gas chromatograph/mass spectrometer system; MFC – mass flow controller; TC – temperature controller; P – pressure sensor; CHXE – cyclohexene; iBU – isobutane)

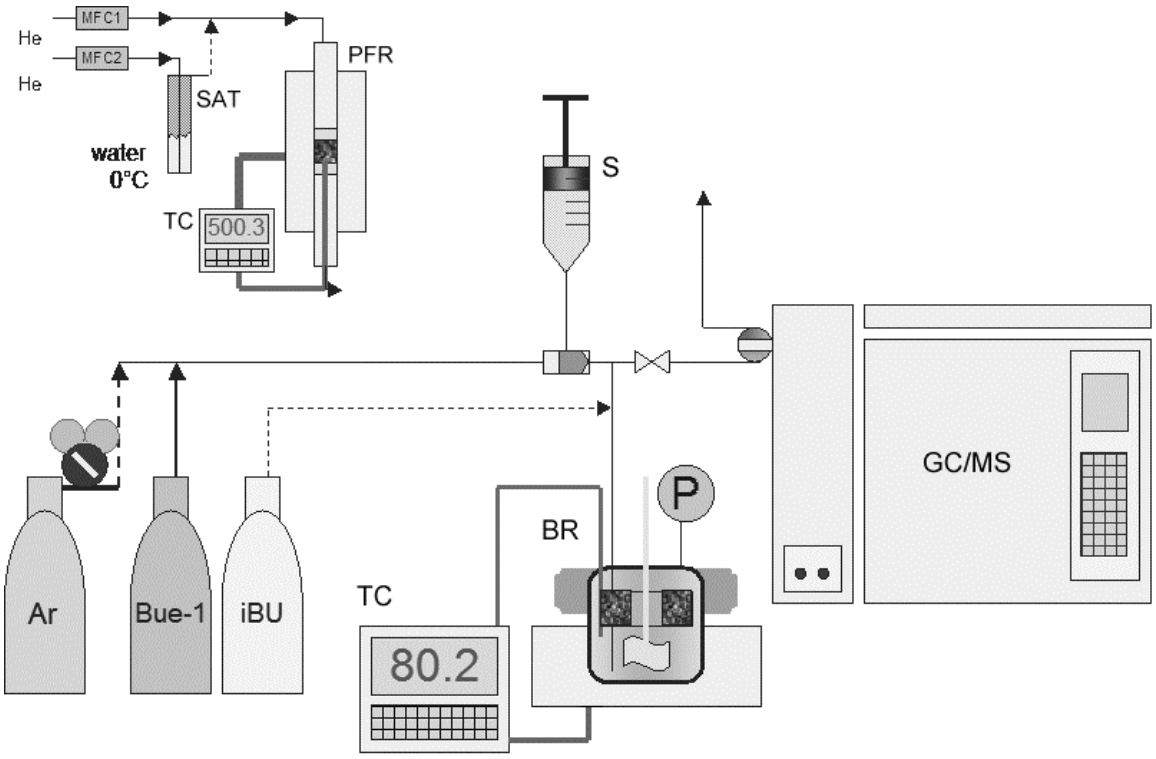


Figure 1.4. Experimental batch reactor setup for the measurement of alkylation activities. (BR – batch reactor setup; S – syringe; GC/MS – gas chromatograph/mass spectrometer system; TC – temperature controller; P – pressure gauge; PFR – plug-flow reactor setup used for activation; SAT – saturator used for water vapor pretreatment of catalysts; MFC – mass flow controller; iBU – isobutane; Bue-1 – 1-butene)

# CHAPTER TWO

# QUANTITATIVE LEWIS/BRÖNSTED RATIOS USING DRIFTS[†]

Alexandru Platon and William J. Thomson[*]

Department of Chemical Engineering,

Washington State University,

Pullman, Washington 99164-2710;

**Abstract**

The extinction coefficient ratio (ECR) of coordinatively bonded pyridine (Lpy) and protonated pyridine (Bpy) was determined in situ by diffuse-reflectance FTIR spectroscopy (DRIFTS), by exposing sulfated zirconia (SZ) containing chemisorbed pyridine to water vapor. Both pure and KBr-diluted SZ samples were analyzed. The linearity with concentration of the Kubelka-Munk transformation was verified for pyridine interacting with the undiluted SZ samples. The portability of published ECR values between transmission and diffuse-reflectance IR spectroscopy, as well as between different types of materials, was found questionable. For the SZ samples analyzed, following a statistical analysis of the data, an Lpy/Bpy ECR value of 2.05 ± 6.3% was determined, resulting in the calculation of an initial Lewis/Brönsted acidity ratio value of 1.1 in the freshly activated material. This ECR determination method should be applicable to other similar solid acids that have a window of relative transparency in the 1600-1400 $cm^{-1}$ range and are capable of retaining chemisorbed pyridine upon exposure to water vapor.

---

[†] Reproduced with permission from *Industrial & Engineering Chemistry Research*, vol. 42 (issue 24, 2003) pages 5988–5992. 

[*] To whom correspondence should be addressed. Tel.: (509)335-8580. Fax: (509)335-4806. E-mail: thomson@che.wsu.edu

*Keywords*: in situ DRIFTS; diffuse-reflectance; Lewis/Brönsted; extinction coefficient ratio; sulfated zirconia.

## 1. Background

Acidity characterization is often performed to measure the density, strength, and type of acid active sites of solid catalysts. Such knowledge helps correlate observed catalyst activity with details from the catalyst preparation stage and provides valuable information for the elucidation of reaction mechanisms. One such acidity characteristic is the surface population distribution of Brönsted and Lewis acid sites. The easiest and most direct method of distinguishing between Brönsted and Lewis acid species is the IR spectroscopy of chemisorbed pyridine.[1-5] Upon interaction with a Brönsted (B) acid, pyridine is protonated and absorbs at a specific IR wavelength around 1540-1545 $cm^{-1}$ (Bpy), as well as at several other specific wavelengths not discussed here. Following interaction with a Lewis (L) acid site, pyridine will also form a coordinatively bonded complex with a specific IR absorption band centered in the range 1449-1452 $cm^{-1}$ (Lpy), along with several other bands. In addition, a band at about 1490 $cm^{-1}$ is common to both species. Depending on the analytical technique, quantification of absolute or relative L/B populations from spectral data involves either the calculation of band absorbances in transmission IR spectroscopy or a Kubelka-Munk (KM) transformation of diffuse-reflectance spectra of powder samples.[6] In transmission spectroscopy, the calculation of absolute concentrations from absorbance band intensities is possible through the Lambert-Beer law. However, in a diffuse-reflectance measurement, such a derivation is restricted to the particular setup used and is usually heavily affected by errors caused by nonrepeatability in particle size and packing density between different samples.[7,8] Error margins of as much as 10% are reported,[8] although a comparable error range is also frequent in transmission IR data (e.g. calculation of molar absorption coefficients[9]).

It is particularly common with the diffuse-reflectance technique that the acidity type repartition be presented in terms of L/B population ratios rather than absolute concentrations. Either from absorbance data or from KM-transformed diffuse-reflectance data, the L/B concentration ratio can be derived from the integrated band intensity ratio ($I_{LPy}/I_{BPy}$) and a previous knowledge of the extinction coefficient ratio (ECR), defined here as the ratio between the proportionality factors, $\varepsilon$, that relate the specific band intensities $I$ with the corresponding concentrations $c$, that is,

$$\frac{c_L}{c_B} = \frac{L}{B} = \left(\frac{I_{Lpy}}{I_{Bpy}}\right)\left(\frac{\varepsilon_{Bpy}}{\varepsilon_{Lpy}}\right) = \left(\frac{I_{Lpy}}{I_{Bpy}}\right)\frac{1}{ECR} \qquad (1)$$

The Kubelka-Munk transformation of diffuse-reflectance ($R$) data is typically performed to linearize band intensities with respect to chromophore concentration. Using diffuse-reflectance FTIR spectroscopy (DRIFTS), the reflectance data, $R$, are usually obtained by ratioing the intensity measured from the sample to that measured from a powder material with a near-ideal reflectance. KBr powder background spectra are generally preferred as ratio background data. This transformation takes the form:

$$KM = \frac{(1-R)^2}{2R} = 2.303\left(\frac{a}{s}\right)c = \varepsilon c \qquad (2)$$

where $a$ is the IR molar absorbtivity, $c$ is the concentration, $s$ is the scattering factor, and $\varepsilon$ is the extinction coefficient

Therefore, L/B values derived from diffuse-reflectance spectra can still be related to molar extinction coefficients ($a$), which, when integrated across each absorption band, are

routinely used in interpreting transmission spectroscopy data. For diffuse-reflectance spectra of chemisorbed pyridine interacting with the solid acid sample, the ECR can be derived from

$$\frac{L}{B} = \left(\frac{KM_{Lpy}}{KM_{Bpy}}\right)\left(\frac{a_{Bpy}}{a_{Lpy}}\right)\left(\frac{s_{1495}}{s_{1545}}\right) = \left(\frac{KM_{Lpy}}{KM_{Bpy}}\right)\frac{1}{ECR} \qquad (3)$$

where the values of *KM*, *a* and *s* are integral across the corresponding absorption band. If the scattering factor (*s*) is not strongly frequency-dependent (so that $s_{1495} / s_{1545} \approx 1$), ECR values derived from transmission IR data can also be used to estimate L/B values from diffuse-reflectance IR data. Moreover, the assumption that extinction coefficients are not influenced by the environment set by the solid acid also has to be made when importing extinction coefficients or their ratio from one material to another.

Corma[10] recommends the general use of published extinction coefficients for the estimation of Brönsted and Lewis acid site populations. These published values are typically obtained by one of the following transmission IR-coupled methods: selective elimination of Brönsted acidity followed by water vapor exposure;[5,11,12] dosing of known amounts of pyridine;[9,13,14,15] or water vapor exposure to convert Lewis acidity into Brönsted acidity.[16] For DRIFTS measurements, pyridine dosing in parallel with thermogravimetric measurements have been reported by Chen et al.[8] However, the ECR values from published data vary widely (Table 1), and there is little agreement even for the same type of IR setup or material. Thus, the portability of these values from one material to another, or from transmission to diffuse-reflectance spectroscopy might be questionable. For example, in a spectrum where the Lpy and Bpy intensities are in a ratio of 1:1, the calculated L/B ratio could range anywhere between 0.3 and 1.8, or even as high as 8.8, when the published ECR values are used.

In this study, an attempt has been made to evaluate a simple method for determining a most probable ECR value, using pyridine as an acidity probe in an in situ diffuse-reflectance FTIR apparatus. The method has been applied to sulfated zirconia (SZ), utilizing a technique where chemisorbed pyridine is first exposed to water vapor and then subjected to dehydration to interconvert the Lpy and Bpy species. This method employs single sample packings and thus avoids variations in the scattering factor, which is strongly dependant on packing density and particle size.[6,17] SZ was considered a good choice to test the method because it has a window of relative transparency in the 1400-1600 $cm^{-1}$ range ($R \approx 45\%$, KM $\approx 0.34$) and, therefore, the undiluted powder is suitable for KM treatment, as is expected to yield linearity with respect to concentration and limited distortions caused by specular reflection.[17] However, this method should be suitable for use with any optically similar solid acid in which water does not completely dislocate chemisorbed pyridine molecules. By avoiding KBr dilution, which is usually recommended,[18] reflectance is maintained in a range where errors inherent to KM in DRIFTS systems are minimal.[7] Also, SZ proved to have very labile Brönsted sites that can easily and reversibly be converted to Lewis sites.[19-22] Another factor in choosing sulfated zirconia is that its surface acidity has recently been a subject of controversy,[23] with some authors considering it superacidic while others measuring, at most, sulfuric acid-like acidity. In addition, the contribution of the Lewis or Brönsted acidity to catalytic activity has also been a subject of divergence[23] as a knowledge of the L/B proportion can be of critical importance in optimizing catalyst activity. For example, Li and Gonzalez[22] concluded that the optimum L/B ratio for n-butane isomerization over SZ was 2.0 (pyridine DRIFTS), although this conclusion was based on a method and parameter values originally developed for silica-alumina in transmission spectroscopy.[11]

## 2. Experimental Section

### *2.1. Equipment and Materials*

Spectra were collected with a Perkin-Elmer System 2000 FTIR single-beam spectrometer using a liquid-nitrogen-cooled MCT detector. Pyridine and water vapor adsorption were carried out in a Harrick Scientific HVC-DR2 reaction chamber with a detachable NaCl window dome, mounted inside a Harrick DRA-2 Praying Mantis diffuse-reflectance accessory designed to minimize parasite specular reflectance. The reaction chamber is capable of heating a 4-mm-thick powder sample to more than 600°C in controlled, flow-through atmospheres, with the temperature measured at the center of the sample. Spectra were collected in the 4000-1000 $cm^{-1}$ interval with a resolution of 4 $cm^{-1}$, obtained by automatically adding 100 scans. However, the frequency interval of focus was the SZ transparency window of 1600-1400 $cm^{-1}$.

Pyridine was obtained from Fisher Scientific (99.9%) and was stored over type 3A molecular sieves (4-8 mesh beads from Acros Organics) to provide a moisture-free pyridine source. Ultrahigh purity helium was obtained from Air Liquide and was passed through desiccant packs of Drierite and molecular sieve 3A to eliminate acquired moisture contamination. The sulfated zirconia was prepared in our laboratory using established synthesis techniques. Synthesis details and material characteristics are reported elsewhere.[24,25]

### *2.2. Procedures*

Test-tube-sized saturators with pyridine (also over molecular sieve 3A desiccant beads) and water were placed in ice baths, purged with helium to eliminate air, and left overnight to equilibrate. SZ and KBr were ground separately, depending on the sample size, for 5-10 min with an agate mortar and pestle, and placed overnight in an oven at 120 °C, along with the detachable

reaction chamber window dome. This grinding procedure was previously shown to yield particle sizes up to 40 $\mu$m.[26] The linearity in concentration of the Kubelka-Munk function was previously shown to hold when particle sizes in the powder sample are smaller than ~7λ,[27] where λ is the IR radiation wavelength. For the 1400-1600 $cm^{-1}$ wavelength interval considered here, the maximum acceptable particle size was ~275 μm. For a separate series of samples, preparations of 10% SZ dispersed in KBr were obtained by weighing the necessary quantities from each previously ground material and then mixing the powders intimately for 1 min in a glass vial placed in a SpectroMill (Chemplex Ind.) impact grinder.

Measurements were performed separately on KBr and SZ. Powder samples were loaded with minimum packing in the DRIFTS sample cup, in repeated sweeps performed with a specially designed tool from Harrick, until the powder surface was free of visible defects. The heating and cooling rates were set to 10°C/min to prevent degradation of the powder surface by uneven thermal expansion. A constant helium flow of 25 sccm, passing through the reaction chamber and powder sample at atmospheric pressure, was maintained for the entire duration of the experiments. KBr powders were dehydrated in situ at 350 °C for 1 h, prior to the collection of background reference spectra at 25°C. Pure SZ and 10% SZ/KBr samples were activated under the same conditions.

Following activation, with the SZ sample temperature held at 150°C, approximately 650 Pa of pyridine vapor was admitted to the reaction chamber for 30 min, by diverting the helium flow through the corresponding saturator. Subsequently, physisorbed pyridine was allowed to desorb for one h at 150°C under helium flow, before the temperature was lowered to 25°C. Spectra of chemisorbed pyridine were then collected at this temperature. These “initial” spectra, as well as all subsequent spectra, were collected as total energy counts and separately ratioed against the KBr total energy reference scans to obtain relative reflectance spectra.

After the initial spectra had been collected, approximately 630 Pa of water vapor was admitted to the reaction chamber in a similar manner, and the SZ samples were held at 25°C for 30-60 min. Initially, spectra were recorded during hydration to ensure that the samples were not reaching saturation and to verify the linearity of the hydration data. After the flow had been switched back to pure inert, the SZ samples were allowed to slowly dehydrate in the dry inert flow, and spectra were recorded every 10 min for 3-4 h. A similar procedure was used for the 10% SZ/KBr samples. Relative reflectance spectra were subsequently subjected to the KM transformation and integrated between 1565 and 1510 $cm^{-1}$ (Bpy) and 1465-1424 $cm^{-1}$ (Lpy). Initial spectral data, as well as spectra at the end of each hydration step, were then used to determine the ECR.

## 3. Results and Discussion

### *3.1. Reversibility of the Lpy-Bpy Interconversion*

A first step in the study was testing the reversibility of L-B interconversion upon hydration and dehydration, performed on single sample packings in the in situ DRIFTS setup. In this way, errors introduced by variable scattering factors from one sample packing to another were avoided. By simply measuring and plotting initial Lpy and Bpy peak areas, as well as peak areas measured during the hydration and dehydration steps, both the linearity of the KM transformation with respect to concentration and the persistence of chemisorbed pyridine can be probed, assuming that undesirable KM-concentration nonlinearities and pyridine loss do not cancel each other.

Previous reports indicate that, upon water vapor exposure of chemisorbed pyridine on SZ, hydrogen-bonded pyridine can be detected.[20] The presence of such a species could affect the

quantification of the Lpy and Bpy species. Therefore, absolute energy spectra taken before and after 60 min of water adsorption at 25°C were ratioed and compared with reflectance spectra of pyridine vapors in contact with SZ at the same temperature. These results are shown in Figure 1, where emerging species in the ratio spectrum, B, should be characterized by downward bands. As can be seen, only slight curvature distortions, corresponding to the strongest features common to physisorbed or hydrogen-bonded pyridine (spectrum A), can be observed. It can therefore be concluded that only minor pyridine dislocation occurs under these conditions.

Data from three repeated linearity tests are merged in Figure 2. Comparing the lines connecting the initial and final hydration points with the dehydration points, it can be concluded that the general trend of Lpy and Bpy band evolution during the dehydration step is to linearly recover the initial L/B distribution. The deviations from linearity during dehydration were found to be associated with interference attributed to gaseous water. Neither at the beginning nor at the end of the hydration step was any immediate, noticeable change observed in this interference. Therefore, it was concluded that the low water concentration under the very short optical length of the DRIFTS reaction chamber could not be the source of the interference. This interference is more likely due to ambient water vapor and the much longer optical length of the internal optical compartment or the sample chamber of the FTIR instrument. It was noticed that the most frequent positive deviations from the linear trend were associated with a decrease in the water interference signal. This phenomenon could therefore be explained by a slow desiccation process, i.e., water vapor admitted to the instrument during the initial experimental setup being slowly absorbed by the desiccant packs.

Rather frequently, this interference observed during the course of the slow dehydration process caused significant error in absorption band quantification. Therefore, data collected over such a long interval was deemed to be unreliable for an ECR calculation, especially when ratioed

against a KBr background obtained separately at a time interval of at least 2 h. The next logical approach was to use the data corresponding to the initial, dry pyridine/SZ and the hydrated pyridine/SZ data points and to statistically determine the most probable Lpy-Bpy slope. These sets of data points were recorded no more than 1 h apart, so that the probability of environmental variations and distortion was greatly diminished.

*3.2. ECR Determination*

In the absence of pyridine loss during the hydration process, it is expected that Lpy species convert into Bpy with a 1:1 stoichiometry. Therefore the decrease in the Lpy concentration should equal the increase in the Bpy concentration. Referring to eq. 3, it is obvious that the slope of a $KM_{Lpy}/KM_{Bpy}$ plot is the negative of the extinction coefficient ratio ECR. In Figure 3, 15 pairs of dry/hydrated pyridine data points for undiluted SZ are compared with 3 paired data points obtained for 10% sulfated zirconia in KBr. Further evidence of the linearity of the KM transformation for spectra on undiluted SZ is the obvious parallelism between the two trends.

In Figure 3, the "tangential" spread (T) is most probably due to the nonrepeatability in the initial degree of dehydration of SZ, whereas the "radial" spread (R) is caused by nonrepeatability in the packing (and therefore in the optical density) of the powder samples. Because these nonrepeatability sources should affect not the slope (ECR) but rather the absolute positions of the Lpy/Bpy data points taken before and after hydration, a statistical analysis was performed on the set of ECR values calculated from each pair of initial/hydrated data points. Using all the available data for both undiluted (16 values) and diluted (5 values) SZ, the mean ECR was found to be 2.22 ± 0.31, within a 95% confidence interval, that is, with an error of ± 14%. However, after elimination of a few outliers detected graphically in the run sequence plot, the most probable

ECR estimate was 2.05 ± 0.13 with 95% confidence (or a ± 6.3% error). The L/B concentration ratio calculated from this ECR value for the set of dry, initial SZ sample spectra was 1.11 with a 95% confidence interval of ±11.3%, and after the statistical removal of two outliers, the L/B ratio was 1.09 ±4.5%. The tangential data spread in Figure 3 indicates that this initial L/B ratio might have been affected by reproducibility in the dehydration procedure or by accidental pyridine contamination with water. Horr et al.[7] have demonstrated that the KM transformation of reflectance spectra is characterized by a propensity to amplify any fluctuations in an FTIR instrument response. Because there were evident fluctuations in the ambient water vapor background in these experiments, the spread in the calculated L/B values might also include such artifacts from the KM treatment.

Although the portability of published extinction coefficient values was suggested,[10] the spread and disagreement in the calculation of this quantity is not uncommon. Examples for both transmission IR and DRIFTS data for pyridine adsorbed on solid acids are listed in Table 1. Proper ECR data for pyridine/SZ, especially in diffuse-reflectance IR spectroscopy, is scarce, and therefore, the use of values obtained from transmission IR spectroscopy on different materials might be questionable. As an example, the specific pyridine ring vibration mode, 19b, is responsible for *both* the Lpy and Bpy bands at rather very different frequencies.[1] This points to the fact that the environment has a decisive influence upon the energy of oscillation. As suggested by the fact that most reported ECR values differ from unity, the extinction coefficients differ between Lpy and Bpy species for this vibration mode. That is, the type and strength of interaction between pyridine and the acid site should affect both the wavenumber and extinction coefficient. For the different materials utilized in published reports, band frequencies for the same vibration mode have shown a slight but noticeable spread (1540-1550 $cm^{-1}$ for Bpy and 1450-1455 $cm^{-1}$ for Lpy.)[5, 8, 9, 11-16,22,28,29] This observation, along with the ECR values listed in Table 1, suggests that

the environment, i.e., the material type and acid strength, should and does exert an influence upon the ECR values. Moreover, the scattering factor, which determines the correlation between concentration and KM band intensity, could very well be frequency-dependent.

In light of this reasoning, it is not surprising that the ECR value calculated here differs from values reported in previous works. The data acquired in this study suggests that ECR and extinction coefficient data are not portable from one material to another and/or from one IR technique to another.

*References:*


(1) Cook, D. Vibrational Spectra of Pyridinium Salts. *Can. J. Chem*. **1961**, *39*, 2009.

(2) Gill, N. S.; Nuttall, R. H.; Scaife, D. E.; Sharp, D. W. A. Infrared Spectra of Pyridine Complexes and Pyridinium Salts. *J. Inorg. & Nuclear Chem*. **1961**, *18*, 79.

(3) Zerbi, G.; Crawford, B., Jr.; Overend, J. Normal Coordinates of The Planar Vibrations of Pyridine and its Deuterioisomers [Determined] with a Modified Urey-Bradley Force Field. *J. Chem. Phys*. **1963**, *38*, 127.

(4) Parry, E. P. An Infrared Study of Pyridine Adsorbed on Acidic Solids. Characterization of Surface Acidity. *J. Catal.* **1963**, *2*, 371.

(5) Basila, M. R.; Kantner, T. R.; Rhee, K. H. The Nature of the Acidic Sites on a Silica-Alumina. Characterization by Infrared Spectroscopic Studies of Trimethylamine and Pyridine Chemisorption. *J. Phys. Chem*. **1964**, *68*, 3197.

(6) Fuller, M. P.; Griffiths, P. R. Diffuse-reflectance Measurements by Infrared Fourier Transform Spectrometry. *Anal. Chem.* **1978**, *50*, 1906.

(7) Horr, T. J.; Ralston, J.; Smart, R. St. C. Methods for Quantitative Diffuse-reflectance FT-IR: Adsorption Densities of Alcohols on Silica Powders. *Collois. Surf.* **1992**, *64*, 67

(8) Chen, D.; Sharma, S.; Cardona-Martínez, N.; Dumesic, J. A.; Bell, V. A.; Hodge, G. D.; Madon, R. J. Acidity Studies of Fluid Catalytic Cracking Catalysts by Microcalorimetry and Infrared Spectroscopy. *J. Catal.* **1992**, *136*, 392.

(9) Emeis, C. A. Determination of Integrated Molar Extinction Coefficients for Infrared Absorption Bands of Pyridine Adsorbed on Solid Acid Catalysts. *J. Catal*. **1993**, *141*, 347.

(10) Corma, A. Inorganic Solid Acids and Their Use in Acid-Catalyzed Hydrocarbon Reactions. *Chem. Rev.* **1995**, *95*, 559.

(11) Basila, M. R.; Kantner, T. R. The Nature of the Acidic Sites on Silica-alumina. A Reevaluation of the Relative Absorption Coefficients of Chemisorbed Pyridine. *J. Phys. Chem.* **1966**, *70*, 1681.

(12) Rosenthal, D. J.; White, M. G.; Parks, G. D. Estimating the Relative Acid Site Density of Silica-alumina by Infrared Spectroscopy Using a Selective Reactant Poison. *AIChE J.* **1987**, *33*, 336.

(13) Hughes, T. R; White, H. M. A Study of the Surface Structure of Decationized Y Zeolite by Quantitative Infrared Spectroscopy. *J. Phys. Chem.* **1967**, *71*, 2192.

(14) Datka, J.; Turek, A. M.; Jehng, J. M.; Wachs, I. E. Acidic Properties of Supported Niobium Oxide Catalysts: An Infrared Spectroscopy Investigation. *J. Catal.* **1992**, *135*, 186.

(15) Guisnet, M.; Ayrault, P.; Datka, J. Acid Properties of Dealuminated Mordenites Studied by IR Spectroscopy. 2. Concentration, Acid Strength and Heterogeneity of OH Groups. *Pol. J. Chem*. **1997**, *71*, 1455.

(16) Matulewicz, E. R. A.; Kerkhof, F. P. J. M.; Moulijn, J. A.; Reitsma, H. J. Structure and Activity of Fluorinated Alumina. 1. Determination of the Number of Protonic Sites by an Infrared Study of Adsorbed Pyridines. *J. Colloids Interf. Sci.* **1980**, *77*, 110.

(17) Delgass, W. N.; Haller, G. L.; Kellerman, R.; Lunsford, J. H. *Spectroscopy in Heterogeneous Catalysis*; Academic Press: New York, 1979.

(18) Smith, B. C. *Fundamentals of Fourier Transform Infrared Spectroscopy*; CRC Press: Boca Raton, FL, 1996.

(19) Arata, K. Solid Superacids. *Adv. Catal.* **1990**, *37*, 165 .

(20) Morterra, C.; Cerrato, G.; Bolis, V. Lewis and Brönsted Acidity at the Surface of Sulfate-doped $ZrO_2$ Catalysts. *Catal. Today* **1993**, *17*, 505.

(21) Zhang, C.; Miranda, R.; Davis, B. H. Platinum-sulfated-zirconia. Infrared Study of Adsorbed Pyridine. *Catal. Lett.* **1994**, *29*, 349.

(22) Li, B.; Gonzalez, R. D. In Situ DRIFTS Study of the Deactivation and Regeneration of Sulfated Zirconia. *Catal. Today* **1998**, *46*, 55.

(23) Davis B. H.; Keogh, R. A.; Srinivasan, R. Sulfated Zirconia as a Hydrocarbon Conversion Catalyst. *Catal. Today* **1994**, *20*, 219.

(24) Chellappa, A. S.; Miller, R. C.; Thomson, W. J. Supercritical Alkylation and Butene Dimerization over Sulfated Zirconia and Iron-manganese Promoted Sulfated Zirconia Catalysts. *Appl. Catal. A: Gen.* **2001**, *209*, 359.

(25) Gore, R. B.; W. J. Thomson, W. J. Pulsed Gas-phase Alkylation of Isobutane/2-Butene over Sulfated Zirconia. *Appl. Catal. A: Gen.* **1998**, *168*, 23.

(26) Gore, R. B. Surface Acidity and Catalytic Activity of Sulfated Zirconia. Ph.D. Dissertation, Washington State University, Pullman, WA, 1997.

(27) Mandelis, A.; Boroumand, F.; van den Bergh, H. Quantitative Diffuse-reflectance and Transmittance Spectroscopy of Loosely Packed Powders. *Spectrochim. Acta* **1991**, *47A*, 943.

(28) Take, J.; Yamaguchi, T.; Miyamoto, K.; Ohyama, H.; Misono, M. Brönsted Site Population on External and on Internal Surface of Shape-Selective Catalysts. *Stud. Surf. Sci. Catal.* **1986**, *28*, 495.

(29) Davis, B. H.; Keogh, R. A.; Alerasool, S.; Zalewski, D. J.; Day, D. E.; Doolin, P. K. Infrared Study of Pyridine Adsorbed on Unpromoted and Promoted Sulfated Zirconia. *J. Catal.* **1999**, *183*, 45.

Table 1. Published ECR values for Lpy/Bpy species of pyridine interacting with solid acids

| technique | ECR | material | ref |
|---|---|---|---|
| transmission IR | 8.8 | silica-alumina | 5[a] |
| | 1.8 | silica-alumina | 11[b] |
| | 0.96-1.33 | zeolite Y | 13 |
| | 1.15 | HZSM-5, montmorillonite cross-linked with $ZrO_2$ and $Al_2O_3$ | 28 |
| | 1.1 | H-mordenite (Bpy) and alumina (Lpy) | 15 |
| | 0.8-1.0 | fluorinated alumina | 16 |
| | 1.52 | HY zeolite (Bpy) and alumina (Lpy) | 14 |
| | 0.98-1.80 | several zeolites, silica-aluminas | 9 |
| DRIFTS | 1.4[c] | USY and silica-alumina | 8 |
| | 1[d] | unpromoted and promoted sulfated zirconia | 21, 29 |
| | 0.3-0.4[e] | sulfated zirconia | 22 |

[a] Calculation based on parameters confirmed by Rosenthal et al.[12]

[b] Recalculation of earlier data.[5]

[c] Peak areas reproducible to within 10%.[8]

[d] ECR value assumed, and used, with absorbance units.[21,29]

[e] Calculated from L/B values and peak areas of reported spectra.

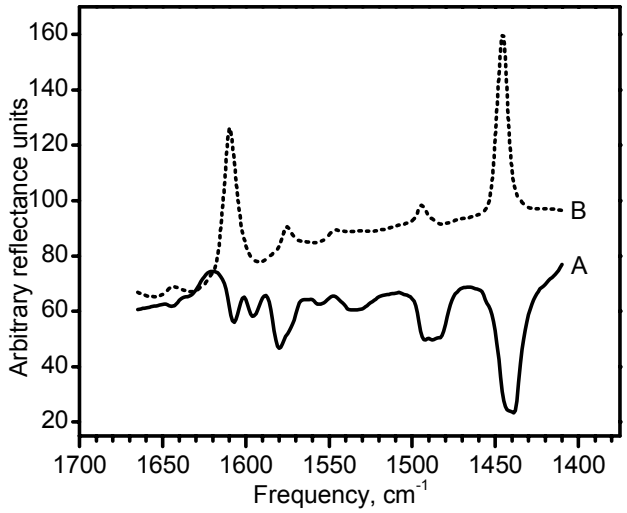


Figure 1. (A) Reflectance spectrum of pyridine vapor in contact with SZ at 25°C for 30 min, showing features characteristic of physisorbed pyridine at 1439, 1483, 1488, 1580, 1596, and 1607 $cm^{-1}$. (B) Ratio between absolute spectra of SZ-chemisorbed pyridine after and before hydration for 60 min at 25°C.

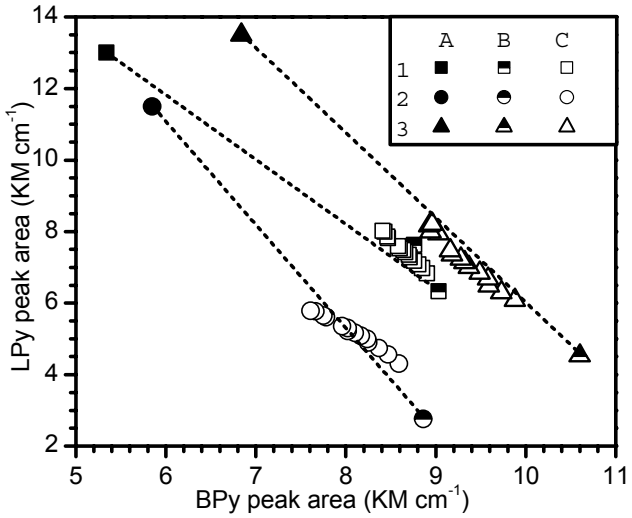


Figure 2. Linearity test for pyridine/SZ hydration/dehydration at 25 °C, for 3 experiments. (A) initial points, (B) data taken during and at the end of the 60-min hydration, (C) data taken during the 4–h dehydration in dry He flow. (Dotted lines are qualitative.)

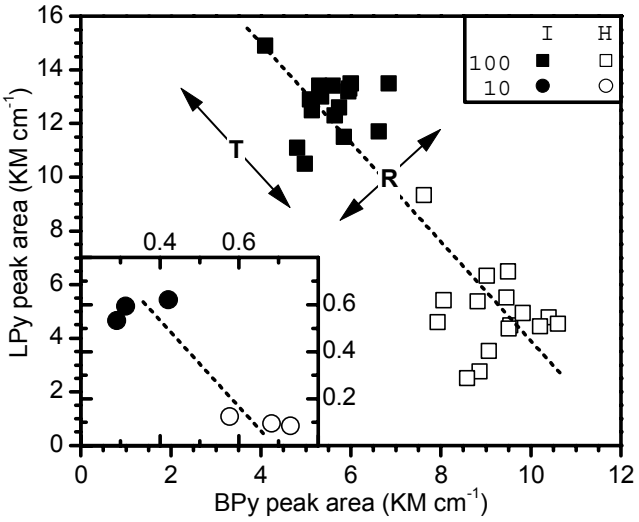


Figure 3. Comparison between undiluted- and diluted-SZ hydration of pyridine chemisorbed on Lewis and Brönsted sites: (I) initial, dry pyridine/SZ; (H) hydrated pyridine/SZ; (100) undiluted SZ; (10) 10% SZ dispersed in KBr. (dotted lines are qualitative.)

# CHAPTER THREE

# LOW-TEMPERATURE TEST REACTION FOR HYDRIDE TRANSFER ON SOLID ACID CATALYSTS

Short title: Hydride transfer test

Alexandru Platon and William J. Thomson*

Department of Chemical Engineering,

Washington State University,

Pullman, WA 99164-2710;

**Abstract**

A new model test reaction is proposed for the estimation of low-temperature hydride transfer (HT) activity of solid acids. The reaction of cyclohexene with isobutane on zeolite Beta, ZSM-5 and sulfated zirconia distinguished between disproportionation/hydrogen transfer and HT. The effects of acid site density, catalyst structure and interaction with isobutane are discussed.

Keywords: hydride transfer; hydrogen transfer; isobutane; alkylation; cyclohexene; solid acid catalyst; zeolite Beta; sulfated zirconia; ZSM-5.

* To whom correspondence should be addressed. Tel.: (509)335-8580, Fax: (509)335-4806, E-mail: thomson@che.wsu.edu

## Introduction

Hydride transfer is a significant process that accompanies most solid-acid-catalyzed reactions of hydrocarbons. During low temperature reactions at which cracking becomes slower than oligomerization, hydride transfer has been found to be responsible for limiting the buildup of carbonaceous deposits that block catalyst active sites [1,2], as well as for determining the catalyst lifetime and product distribution in the solid-acid catalyzed alkylation of isobutane with light olefins (see for ex. [3,4,5]). The process employs the bimolecular transfer of a hydride ion from a donor species to an acceptor species. On acid active sites, acceptors are carbenium-type carbocations and, following the hydride ion transfer, they desorb as neutral hydrocarbons, while a new carbocation is formed from the donor (Reaction 1).

$$R^{(+)} + R'\text{-}H \rightarrow R\text{-}H + R'^{(+)} \qquad (1)$$

If both the acceptor and the donor are found in a chemisorbed state before the transfer occurs, similar to a Langmuir-Hinshelwood surface reaction model, a net transfer of hydrogen from the donor to one or more acceptors can occur, along with a buildup of the remaining carbon-rich deposits on the catalyst. This particular case is usually termed hydrogen transfer [6]. Situations also exist when a transfer between identical chemisorbed species results in a simple disproportionation. Disproportionation, however, can also be an initial step in the hydrogen transfer process when the resulting carbenium product undergoes oligomerization and dehydrogenation faster than it desorbs. Therefore, these two cases will be referred together to as disproportionation and/or hydrogen transfer (DHGT).

A contrasting case is that of hydride ion transfer from a physisorbed donor to a chemisorbed acceptor as described by the Rideal surface reaction model. This process can be viewed as a chain

transfer reaction where the resulting carbocation can continue a series of reactions such as olefin addition, isomerization and cracking. It is this latter particular hydride transfer (HT) case that this work will focus on.

Few methods have been reported to date for the evaluation of the HT activity of solid acids, and these methods are based on the knowledge gained from the study of hydrocarbon cracking reactions on solid acids. Thus, the method devised by Lukyanov [7] is based on the interpretation of the product distribution obtained from the decomposition of n-hexane at 400 °C in the presence of the catalyst of interest. The particular HT product that is monitored is isobutane, produced via a process depicted in Reaction 2:

$$\text{n-}C_6 + i C_4^{(+)} \rightarrow C_6^{(+)} + i C_4 \qquad (2)$$

However, there are a number of issues that affect the applicability of this model reaction to lower temperature conditions such as the alkylation process [8].

During alkylation of isobutane with light olefins, HT is directly responsible for the formation of the desired gasoline-range isoalkanes. For example, in the alkylation of isobutane with butene the occurrence of HT from feed isobutane to a chemisorbed isooctyl carbenium ion results in the formation of the desired isooctane product while the isobutyl carbenium ion produced undergoes olefin addition to recover the $C_8$ carbocation (Reactions 3 and 4):

$$i C_4 + C_8^{(+)} \rightarrow i C_4^{(+)} + C_8 \qquad (3)$$

$$i C_4^{(+)} + C_4^{=} \rightarrow C_8^{(+)} \qquad (4)$$

The hydride transfer from isobutane in Reaction 3 is the key step that controls the alkylation process, and therefore it is opposite of Reaction 2 where isobutane is a reaction product. Moreover, the extrapolation of measured HT activities from 400 °C to the much lower temperatures typical of alkylation could prove ineffective in describing the behavior of the catalyst of interest when activation energies of the simultaneous elementary processes are very different.

It was therefore found necessary to devise a test method capable of more accurate measurements of HT activity at low temperatures that are meaningful for the study of processes such as the solid-acid catalyzed isobutane/olefin alkylation. In addition to its ability to quantitatively measure HT, further considerations of utility as a model test reaction included simplicity and unsophisticated reaction product analysis.

Since cyclic hydrocarbons are relatively reluctant to cracking when compared to normal- or isoalkanes, Cheng and Rajagopalan [9] and Suarez *et al.* [10] have employed cyclohexene to estimate the relative reaction rates of hydrogen transfer, isomerization and other elementary processes. They found that cracking was insignificant at 250 °C on various zeolite catalysts. Chemisorbed cyclohexene (i.e. the cyclohexyl carbenium ion) is comparable in terms of molecular size to the isooctyl intermediate found in alkylation. Moreover, the oligomerization of a bulky cycloolefin such as cyclohexene should be sterically inhibited to a certain degree, especially in the narrow pores of a zeolite.

It was therefore hypothesized in this study that the reaction of cyclohexene in the presence of isobutane, a hydride donor, could prove itself useful in estimating the low temperature hydride transfer activity of solid acids. For the purpose of testing this proposed model reaction, three types of catalysts were considered: zeolites Beta and ZSM-5, and sulfated zirconia. Zeolite Beta

and sulfated zirconia are reported to be active for isobutane alkylation with olefins, which, as stated earlier, is a HT-demanding process [11,12]. At the same time, zeolite ZSM-5 is a narrow-pore cracking catalyst that is known to sterically limit hydride transfer to a greater extent than zeolite Beta [13]. The presumption was made, and tested, that differences in the HT activities of these materials would result in measurable changes in the product distribution from the reaction of cyclohexene and isobutane.

**Experimental**

Samples of zeolite Beta with $SiO_2/Al_2O_3$ ratio values (SAR) of 25 (25BEA) and 75 (75BEA), as well as zeolite ZSM-5 with an SAR value of 80 (80ZSM5), were purchased from Zeolyst (CP814E, lot no. 1822-92; CP811E-75, lot no. 1822-74; CVB8014, lot no. 1822-80, respectively) in a very fine powder form. The 25BEA and the 80ZSM5 zeolites were supplied in the $NH_4$-exchanged form, while the 75BEA was in the acidic form. Sulfated zirconia (SZ) was previously synthesized in our laboratory, as described in an earlier publication [14].

The zeolite powders were converted into their corresponding larger particle size materials by dispersion in colloidal silica (Ludox LS 30 wt.%, d=1.210) to yield a zeolite concentration of approximately 65±1 wt.% in the resulting dry material. The dry material was crushed and sieved, and the particle size cut of 0.59-1.651mm was retained for the subsequent measurements. The corresponding materials were coded 25BEA65, 75BEA65 and 80SZM565, respectively.

Surface area measurements were performed using a Coulter SA-3100 automated characterization machine using the BET method. The catalyst dry weights were determined by heating catalyst samples in a Netzsch STA 409PC/Balzers Quadstar 422 TGA/MS analyzer under a flow of ultra-

pure argon (Air Liquide) up to 1000 °C and then holding at the maximum temperature for one hour. The weight loss for SZ was calculated only up to 650 °C, since above about 700 °C major sulfate loss occurred. Catalyst activation temperature profiles were also identified in the TGA/MS analyzer. For the zeolite samples in their ammonium form, complete decomposition into the acidic form was achieved by holding the temperature at 500 °C for two hours. Under a heating ramp of 10 °C/min, all zeolites showed a major water loss peak between 90-250 °C and a secondary one centered at about 450-500 °C, and therefore activation was considered complete after holding these materials for two hours at 500 °C. The sulfated zirconia samples showed complete activation (as indicated by water evolution) as well as undetectable sulfur loss at 350 °C.

Total acidity measurements were carried out in an ASDI RXM-100 catalyst characterization apparatus. Catalyst samples were loaded into a quartz tube, evacuated for at least one hour at room temperature, and then heated under continuous vacuum up to 130 °C at a rate of 2 °C/min, then up to the activation temperature at a rate of 10 °C/min, whereupon the activation temperature was held constant for two hours. The total and physical adsorption isotherms of ammonia were measured volumetrically at 80 °C for several samples from each catalyst. An overnight evacuation of the sample was performed after every total adsorption isotherm measurement in order to allow physisorbed ammonia to desorb from the catalysts. The chemisorption amounts were calculated for each sample as the difference between the two isotherms in their flat and parallel monolayer regions, normalized to the dry catalyst weight. Total isobutane adsorption capacities were determined using the same apparatus, conditions and activation method, from the total adsorption isotherm of isobutane in contact with samples from each material, by extrapolating the linear monolayer region of each isotherm to a zero equilibrium pressure. Isobutane chemisorption could not be detected at 80 °C.

The reaction tests were performed at atmospheric pressure in a simple quartz plug-flow reactor situated inside a furnace at a controlled temperature. Empty spaces in the reactor were filled with inert material (pyrex wool and glass beads) in order to minimize axial dispersion and mixing transients. Gas flows were controlled using Matheson 8272 mass-flow controllers. Catalyst samples were activated in situ under a constant flow of 20 $STDcm^3$/min (sccm) of UHP helium (Air Liquide). The activation temperature profiles were identical to those used for the total acidity measurements. Following activation, the temperature was lowered to 80 °C and a flow of 20 sccm of isobutane (99%, Matheson) was added to the helium feed for at least 30 minutes. Cyclohexene (≥99.0%, Aldrich) was then added to the feed stream at a rate of 0.371 equivalent sccm, by passing 10 sccm of UHP helium through a saturator containing liquid at 0 °C. The catalyst loadings in the reactor were calculated to yield a constant cyclohexene molar space velocity of 0.208 $min^{-1}$ with respect to the number of catalyst acid sites as determined from the total acidity measurements. The effluent composition was measured by means of a mass spectrometer-coupled gas chromatograph (GC/MS, Hewlett-Packard model GCD G1800A) equipped with a Supelco Supel-Q-Plot capillary column. For each experiment, samples were injected every 3.2 min using an in-line sampling valve during a continuous, isothermal GC analysis at 150 °C. GC peak separation was enhanced by extracting the corresponding characteristic ion fragments for cyclohexane (M/z=80), cyclohexene (M/z=67), methylcyclopentane (M/Z=56) and methylcyclopentene (M/z=67) from the total ion current recorded in the MS. Isobutane concentrations were not quantified; no other products were detected during the experiments.

Control experiments were run for each material with the purpose of testing the cyclohexene disproportionation and/or hydrogen transfer (DHGT) activity when isobutane was absent. Cyclohexene feed concentrations and molar space velocities were maintained identical to the test employing isobutane, by balancing the feed with supplemental helium. Experimental

uncertainties, although not evaluated for these controls, were considered similar to those observed for each material during the hydride transfer tests.

**Results and discussion**

Table 1 summarizes all the measured characteristics for the four materials tested. Aside from the quantities measured directly, surface acid site density and adsorbed isobutane/acid site ratios have been calculated in order to help in the interpretation of the reaction results.

The observed product distribution from the reaction of cyclohexene (CHXE) with isobutane (IBU) included cyclohexane (CHX), methylcyclopentane (MCP) and 1-methylcyclopentene (MCPE). No other $C_4$ hydrocarbons were detected in the product stream. Small traces of bicyclohexyl were detected at the end of the whole experiment series upon reconditioning the GC column at an elevated temperature. The proposed reaction mechanism is represented in Figure 1. It is assumed that CHX is a product of hydride transfer (HT), MCPE a product of isomerization (ISO), while MCP is a product of ISO followed by HT (similar to ref. [9]).

Typical experimental data from the test reaction on 25BEA65 at 80 °C is presented in Figure 2. During all experiments, CHX, MCP and MCPE concentrations have peaked within the first 40 minutes on stream, while CHXE conversions dropped to values lower than the observed noise level in experimental data. Since no $C_4$ hydrocarbon products were detected, it was concluded that once one HT turnover was complete on an active site, the formed $tC_4^+$ carbenium ion completely blocks the active site from participating in any subsequent reaction cycle. While this situation is not suitable for a practical reactor due to the almost instantaneous deactivation of the catalyst, it is however ideal for the purpose of titrating the acid sites active for hydride transfer.

For the purpose of active site titration, HT product formation rates were expressed in terms of turnover frequency (TOF), as moles of cycloalkane products formed per mole of acid site per unit time, although this quantity loses its meaning when applied to transient data. Upon integration of the HT TOF peak with respect to time on stream, the total number of moles of HT products formed on each mole of active sites can be calculated. It was shown above that acid sites undergoing hydride transfer are completely deactivated after one turnover. Indeed, this is in part validated by the fact that the above integral was always smaller than unity for all materials tested, as shown by the results in Figure 3. Therefore, the above integral can be thought of as the apparent fraction of sites active for HT out of the total acid sites that are detected by ammonia chemisorption, or in other words, the acid site availability to hydride transfer (AHT). It was of interest to also estimate the activities for the Rideal-type HT decoupled from the undesired DHGT contributions. Product formation rates measured for each material during the DHGT control experiments ("no IBU" in Figure 3) were subtracted from the data obtained above. Based upon this difference, 25BEA65 fared best in terms of acid site AHT (7.3%), followed closely by 75BEA65 (6.5%) and then by SZ (2.9%). 80ZSM565 seems to completely lack HT activity at 80 °C, but shows a significant DHGT activity as judged by this calculation.

Peak values of HT and ISO turnover frequencies were also compared in Figure 4. While the overall AHT was more elevated on 75BEA65 than on SZ, the peak HT TOF was lower on the 75BEA65. The observed maximum rates could be affected to some degree by the limited diffusion rates in the narrow pores of the zeolite structure, while the overall AHT should be more closely related to the intrinsic activity of the catalysts. SZ as well as both BEA materials showed almost identical DHGT activities, both in terms of percent availability (Figure 3) and peak rates (Figure 4), indicating that the tendency to form polyunsaturated carbonaceous deposits should be similar in all three materials at 80 °C. SZ showed a significantly higher ISO peak rate than the two BEA zeolites, while the higher acid density 25BEA65 was slightly more active for ISO than

75BEA65. The peak isomerization rate was not influenced by the presence or absence of IBU on SZ and 80ZSM565, as the ISO results indicate, while on zeolites Beta, ISO is somewhat inhibited by the presence of IBU. Based on this observation, ring rearrangement isomerization in intermediates on SZ and 80ZSM565 happens much faster than any subsequent HT, DHGT or cycloolefin desorption process.

As expected from the higher aluminum content, a higher ammonia chemisorption amount was measured on 25BEA65 than on 75BEA65. The measured AHT values suggest that within the same type of structure (BEA), the higher acid site density of 25BEA65 improves hydride transfer activity in terms of the apparent number of acid sites involved in HT. This result is to a certain degree in accord with the report from Suarez *et al.* [10] who have found that the hydrogen transfer activity, measured during CHXE conversion at 250 °C on several zeolites, correlates directly with the fraction of paired aluminum sites in the zeolite structure. Following theoretical calculations of carbocations interacting with Si-O-Si and Si-O-Al zeolite-like sites, Mota *et al.* [15] concluded that the carbenium ion resulting from a HT reaction (such as $t\mathrm{C}_4^+$ in the scheme in Figure 1) is better stabilized by the more acidic Si-O-Al site and therefore, the direct mutual proximity of such highly acidic sites should enhance the likelihood of HT reactions.

An intriguing case however is sulfated zirconia. Its surface acid site density as calculated in Table 1 is twice the surface acid density on 25BEA65, yet its hydride transfer activity is 2.5 times lower. A possible explanation of the poor AHT in SZ is its lower adsorption capacity for IBU, as shown in Table 1. Indeed, when compared with 25BEA65, the IBU physisorption amount detected on SZ was 23 times lower when normalized to the dry weight, or 9 times lower when normalized to the number of acid sites. It was shown that the dilution of the hydride donor IBU was detrimental to the formation of HT products during solid-acid catalyzed alkylation [2,16]. An

argument can be made that a catalyst structure capable of adsorbing an increased amount of IBU in the proximity of the active sites should exhibit enhanced HT from the adsorbed hydride donor.

## Conclusion

Little choice exists to date in the estimation of low-temperature activities for hydride transfer (HT) of solid acid catalysts. Methods originally developed to describe high temperature cracking reaction systems could be of little help in conjunction with reactions such as isobutane/olefin alkylation. The reaction between isobutane and cyclohexene is proposed as a test to estimate the HT activity of solid acids at low temperatures. The proposed test easily discerned between disproportionation/hydrogen transfer and isobutane/cyclohexene HT on zeolites Beta, ZSM-5 and sulfated zirconia. Out of the total number of acid sites determined by ammonia chemisorption titration, the apparent fraction available to mediate HT reactions could be estimated. The results obtained for two silica/alumina ratio values in zeolite Beta were found in perfect accord with evidence indicating that denser strong-acid sites enhance the HT process. The lower per-site HT activity measured in the even denser-acid-site sulfated zirconia could be explained by its much lower isobutane adsorption capacity per acid site. Although zeolite ZSM-5 showed significant disproportionation/hydrogen transfer activity, no measurable Rideal-type, low-temperature HT activity was detected for this otherwise successful cracking catalyst.

## Acknowledgements

This work was supported by the O.H. Reaugh Laboratory for Oil and Gas Processing Research at Washington State University. Suggestions for devising the GC analysis procedure were kindly provided by David C. LaMont.

**References**


[1] C. Flego, G. Bellussi, I. Kiricsi, Appl. Catal. A 126 (1995) 401

[2] D.M. Ginosar, D.N. Thompson, K.C. Burch, Appl. Catal. A 262 (2004) 223

[3] F W. Kirsch, J.D. Potts, D.S. Barmby, Proceedings - American Petroleum Institute, Division of Refining 48 (1968) 1000

[4] G.S. Nivarthy, Y. He, K. Seshan, J.A. Lercher, J. Catal. 176 (1998) 192

[5] A. Feller, I. Zuazo, A. Guzman, J.O. Barth, J.A. Lercher, J. Catal. 216 (2003) 313

[6] A. Corma, P.J. Miguel, A.V. Orchillés, Appl. Catal. A 138 (1996) 57

[7] D.B. Lukyanov, J. Catal. 145 (1994) 54

[8] K. Yoo, P.G. Smirniotis, Appl. Catal. A 227 (2002) 171

[9] W.-C. Cheng, K. Rajagopalan, J. Catal. 35 (1993) 483

[10] W. Suarez, W.-C. Cheng, K. Rajagopalan, A.W. Peters, Chem. Eng. Sci. 45 (1990) 2581

[11] K. Hatakeyama, T. Suzuka, M. Yamane, Sekiyu Gakkaishi 34 (1991) 267

[12] A. Corma, M.I. Juan-Rajadell, J.M. Lopez-Nieto, A. Martinez, C. Martinez, Appl. Catal. A 111 (1994) 175

[13] B.G. Anderson, R.R. Schumacher, R. van Duren, A.P. Singh, R.A. van Santen, J. Mol. Cat. A 181 (2002) 291

[14] A.S. Chellappa, R.C. Miller and W.J. Thomson, Appl. Catal. A 209 (2001) 359

[15] C.J.A. Mota, P.M. Esteves, M.B. de Amorim, J. Phys. Chem., 100 (1996) 12418

[16] D.M. Ginosar, D.N. Thompson, K. Coates, D.J. Zalewski, Ind. & Eng. Chem. Res. 41 (2002) 2864

Table 1. Measured and calculated characteristics of the catalysts used in the study. (S.A. – surface area; $iC_4$ – isobutane)

| | dry weight | | BET S.A. | $NH_3$ chemisorption | | | $iC_4$ total adsorption | | |
|---|---|---|---|---|---|---|---|---|---|
| material | wt% | ± % | $m^2$/g(dry) | mmol/g(dry) | ± % | μmol/$m^2$ | mmol/g(dry) | ± % | $iC_4$:acid |
| 75BEA65 | 91.9 | 0.19 | 441 | 0.254 | 7.5 | 0.58 | 0.733 | 0.8 | 2.89 |
| 25BEA65 | 90.5 | 0.01 | 444 | 0.572 | 1.3 | 1.29 | 0.780 | 0.0 | 1.36 |
| SZ | 97.4 | 0.11 | 90 | 0.230 | 1.7 | 2.56 | 0.034 | 10.0 | 0.15 |
| 80ZSM565 | 95.7 | 0.07 | 333 | 0.336 | 5.5 | 1.01 | 0.377 | 1.8 | 1.12 |

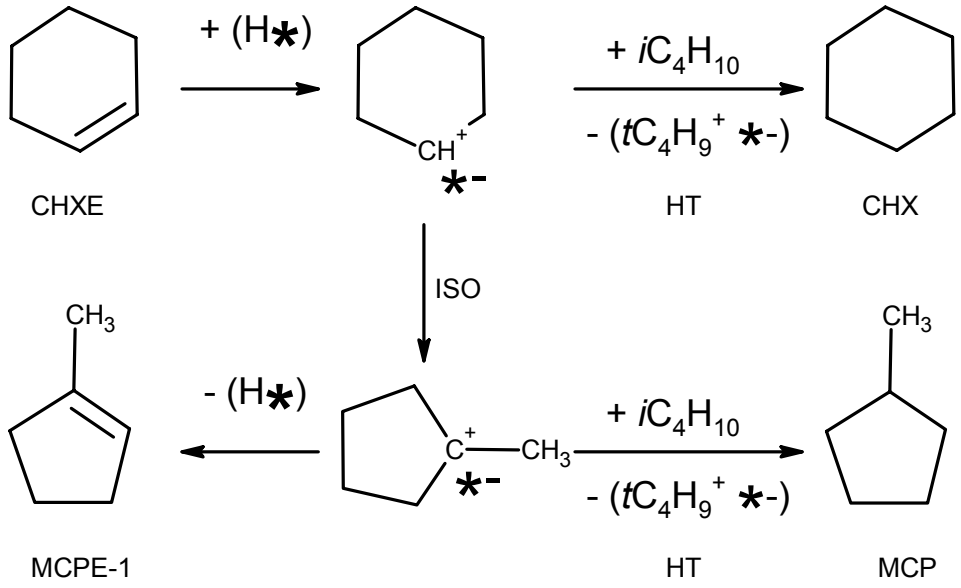


Figure 1. Proposed reaction mechanism. (*) symbolizes an active site.

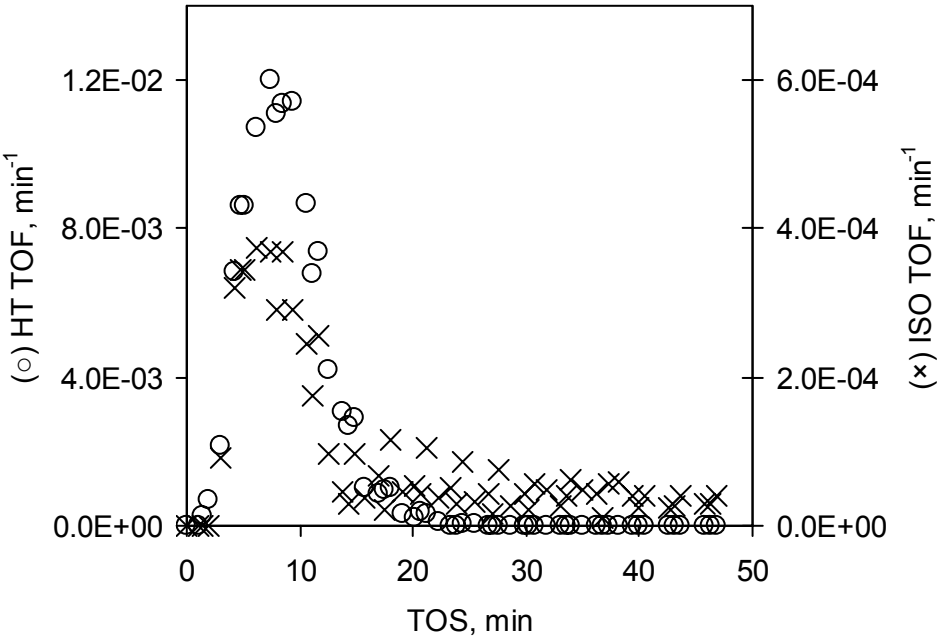


Figure 2. Cumulative data obtained on zeolite 25BEA65 at 80 °C

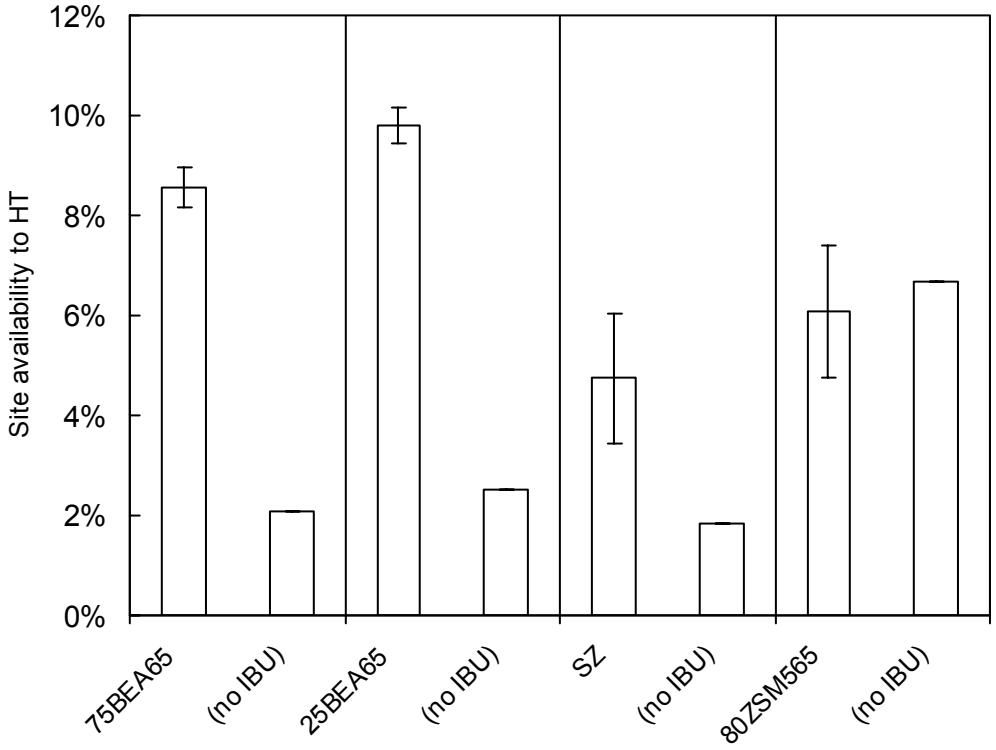


Figure 3. Integrals of HT TOF peaks can be interpreted as a measure of the fraction of the total acid sites that are available for hydride transfer.

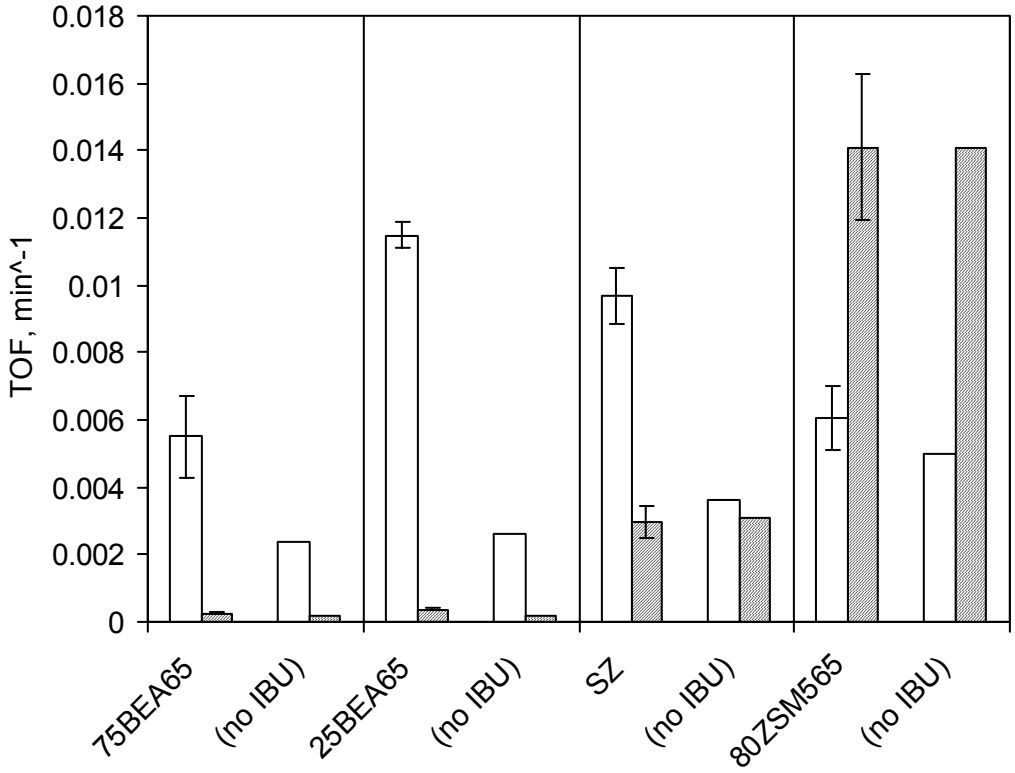


Figure 4. Maximum formation rates recorded for the HT (open bars) and ISO (filled bars) products.

# CHAPTER FOUR

# SOLID ACID CHARACTERISTICS AND ISOBUTANE/BUTENE ALKYLATION

Alexandru Platon and William J. Thomson*

Department of Chemical Engineering,

Washington State University,

Pullman, WA 99164-2710;

**Abstract:**

Catalytic behavior during gas-phase, batch alkylation experiments employing isobutane and 1-butene at 80 °C was studied for Beta zeolites with $SiO_2/Al_2O_3$ (SAR) ratios of 25 (25BEA) and 75 (75BEA), ZSM-5 and sulfated zirconia (SZ). The observed alkylation performance was compared to the low-temperature hydride transfer (HT) activity of the studied catalysts and with their acidity, adsorption capacity and surface area measurements. For all materials studied, a correlation was observed between the measured HT activity and the amount of trimethylpentane (TMP) produced per acid site. The 25BEA catalyst produced the highest amount of trimethylpentane (TMP) and also had the most elevated HT activity. ZSM-5 was found to be inactive for both HT and alkylation, and although SZ had moderate alkylation activity, it also had a higher cracking activity than other materials. Modification by water vapor exposure of 25BEA and SZ did not create any noticeable change in Brönsted acidity, but a dramatic decrease in TMP production was detected on the modified catalysts and explained by competitive adsorption between water and isobutane. The apparent butene conversion correlated well with the total catalyst surface area rather than with the total amount of acid sites. In all the catalysts studied a much stronger interaction with butene than with isobutane was observed, suggesting that

* To whom correspondence should be addressed. Tel.: (509)335-8580, Fax: (509)335-4806, E-mail: thomson@che.wsu.edu

competitive adsorption between the two reactants limits isobutane access to the active sites, resulting in limited hydride transfer.

Keywords: hydride transfer; alkylation of isobutane; butene; cyclohexene; solid acid catalyst; zeolite Beta; sulfated zirconia; ZSM-5.

## 1. Introduction

Alkylate, the refinery product from isobutane alkylation with alkenes, is among the top contributors to the octane number in the typical US gasoline pool. Whereas newer and stricter environmental regulations are expected to increase pressure for the elimination of some of the highest octane rating gasoline components, alkylate is one of the few components that seems to avoid such restrictions [1,2] due to its low volatility, reactivity and toxicity. While alkylate is currently produced by successful commercial refinery processes involving liquid acid catalysts such as sulfuric acid and hydrofluoric acid, increasing efforts are currently concentrated towards finding an alternative solid catalyst that would overcome some of the drawbacks associated with the liquid acids [1,3]. However, the major problem encountered with alkylation on solid acid catalysts is their rapid deactivation.

Numerous efforts have been made to understand the processes responsible for activity and deactivation during alkylation over solid acids. Thus, it is generally agreed that the main alkylation process between isobutane and butene involves Reactions 1-3 listed below. In Reaction 1, butene chemisorbs on an active site (depicted by a star) to form an intermediate butyl carbenium ion. This ion further reacts with another alkene molecule yielding an isooctyl carbenium intermediate, as in Reaction 2. The desired product, isooctane, is formed when the

isooctyl species undergoes a hydride ion transfer from an isobutane molecule, while the butyl carbenium ion is regenerated (Reaction 3).

$$C_4H_8 + *H \rightarrow (C_4H_9)^+ (*)^- \quad (1)$$

$$C_4H_8 + (C_4H_9)^+ (*)^- \rightarrow (iC_8H_{17})^+ (*)^- \quad (2)$$

$$iC_4H_{10} + (iC_8H_{17})^+ (*)^- \rightarrow (tC_4H_9^+) (*)^- + iC_8H_{18} \quad (3)$$

Along with these desired reactions, the carbenium intermediates are involved in side reactions such as multiple olefin addition (oligomerization), molecule chain rearrangement (isomerization), β-scission (cracking), dehydrogenation and subsequent formation of polyenes and polyaromatic hydrocarbons ("coking"). A major, recurring finding among published studies is that hydride transfer (HT) in Reaction 3 is the key process that dictates product distribution and catalyst lifetime [3] during isobutane alkylation. However, few methods have been reported so far for the independent evaluation of the HT activity of solid acids. These methods are usually based on the knowledge gained from the study of hydrocarbon cracking reactions on solid acids. Thus, the method devised by Lukyanov [4] (hexane cracking at 400 °C), and used in some instances to correlate this observed activity with low-temperature alkylation activity [5], is based on Reaction 4 below, which is somewhat opposite to the hydride transfer step in Reaction 3:

$$nC_6H_{14} + (iC_4H_9)^+ \rightarrow (C_6H_{14})^+ + iC_4H_{10} \quad (4)$$

The reaction between cyclohexene and isobutane was reported elsewhere by our group [6] to be capable of measuring low-temperature hydride transfer activities while discriminating between the "true", Rideal-type HT from isobutane (as in Reaction 3) and disproportionation/hydrogen transfer (DHGT) of cyclohexene (similar to the definitions by Corma et al. in ref [7]). This HT test reaction was shown to be able to differentiate among sulfated zirconia, zeolites Beta, and

ZSM-5 (which was inactive for HT), as well as sense the effect of aluminum content on HT in zeolite Beta.

In this study an attempt was made to correlate catalyst performance data for batch alkylation experiments with HT activity as measured by this low-temperature reaction. Furthermore, the effects of the catalytic material, acid site density, catalyst-reactant interaction and catalyst pre-exposure to moisture were investigated. Three different catalytic materials were tested: zeolites Beta and sulfated zirconia, which are known to promote alkylation reactions [8,9], as well as the known cracking catalyst ZSM-5, in which alkylation was found to be limited by its narrow pores [10]. Although gas phase reaction was found to be unfavorable to catalyst stability during alkylation [11], batch gas-phase conditions were chosen for experimental simplicity. Under these conditions, differences in the characteristics and HT activity of the catalysts were expected to yield measurable differences in their $C_8$-range product distribution.

## 2. Materials and experimental procedure

### *2.1. Catalytic materials*

Samples of zeolite Beta with silica/alumina ratios (SAR) of 25 (CP814E, lot no. 1822-92) and 75 (CP811E-75, lot no. 1822-74), as well as zeolite ZSM-5 with an SAR value of 80 (CVB8014, lot no. 1822-80), were purchased from Zeolyst in a very fine powder form and represented here by 25BEA, 75BEA and 80ZSM5, respectively. The 25BEA and the 80ZSM5 zeolites were supplied in the ammonium-exchanged form, while the 75BEA was provided in the acidic form. Sulfated zirconia (SZ) was previously synthesized in our laboratory, and characterization data and synthesis details are given elsewhere [12].

Larger particles of zeolite were prepared by dispersing the fine powders in colloidal silica (Ludox LS 30 wt.%, d=1.210) followed by an overnight drying at 100 °C, to yield a zeolite concentration of approximately 65±1 wt.% in the resulting dry material. The dry material was crushed and sieved, and a particle size cut of 0.59-1.651mm was retained for the subsequent measurements. The corresponding materials are represented here by 25BEA65, 75BEA65 and 80SZM565, respectively.

*2.2. Catalyst characterization*

A Netzsch STA 409PC thermogravimetric analyzer coupled with a Balzers Quadstar 422 mass spectrometer (TGA/MS) was used to measure catalyst dry weights and to determine activation temperature profiles for the catalysts. Catalysts samples were heated with a 10 °C/min rate up to 1000 °C in a flow of ultra pure argon (Air Liquide). Weight losses were used to calculate the dry weights. Because a major sulfur loss occurred in SZ above about 700 °C, its dry weight was based on the weight loss up to 650 °C. Two water losses were detected in the zeolitic materials—a major one between 90-250 °C and a structural water loss at about 450-500 °C. For the ammonium-exchanged zeolites complete ammonia loss occurred by holding the temperature at 500 °C for two hours. It was therefore decided that a complete decomposition/activation is achieved on all zeolites under this latter treatment. Judged from water evolution SZ showed a complete activation at 350 °C.

Surface areas were measured with a Coulter SA-3100 automated characterization machine using the BET method with nitrogen (99.998%, Air Liquide) adsorption data at 77 K. Total acidity and reactant adsorption capacities were determined volumetrically in an ASDI RXM-100 catalyst characterization apparatus. Catalyst samples were activated in a quartz tube under vacuum by being heated 2 °C/min up to 130 °C and then 10°/min up to the activation temperatures determined above which were held constant for two hours. Total ammonia adsorption and

physisorption isotherms at 80 °C were then determined with an intermediate overnight evacuation to desorb physisorbed ammonia. The ammonia chemisorption capacity normalized to the dry catalyst weight was computed by subtracting the two isotherms in their parallel, monolayer segment. Additionally, separate samples from 25BEA65 and 75BEA65 were activated by following the same temperature profile but under a gas stream comprising of 20% oxygen (99.5%, Air Liquide) diluted in helium, and then their dry weights and total acidities were measured. Ammonia chemisorption measurements showed no significant difference in the total acidity of these materials compared to their vacuum/inert-activated counterparts. Separately, isobutane adsorption capacities at 80 °C were determined from the total adsorption isotherm by extrapolating the linear monolayer segment to zero pressure. No isobutane chemisorption was detected in any of the materials tested and thus the isobutane adsorption capacities reported in this work represent physisorbed isobutane. Attempts to measure 1-butene adsorption have consistently failed on all materials because equilibrium pressures could not be reached and the alkene steadily accumulated on the catalysts.

Diffuse-reflectance infrared spectroscopy (DRIFTS) of chemisorbed pyridine was employed to detect and measure Lewis and Brönsted acidity on the catalyst samples. The equipment and materials used were described in detail in ref. [13]. Samples from 25BEA and 75BEA were prepared by diluting portions from the original powdered materials with finely ground KBr (5 minutes with an agate mortar and pestle) to yield 30 wt.% zeolite. SZ powder samples were not diluted in KBr. Samples thus prepared were loaded in the sample cup of the DRIFTS apparatus, then a flow of 25 STD$cm^3$/min (sccm) UHP helium (further desiccated through drierite/molecular sieve 3A) was established for the whole duration of the measurement. Samples were activated in situ at 500 °C for two hours (zeolites) or 350 °C for one hour (SZ). Some of the 25BEA65 and SZ samples were then cooled to 25 °C, exposed to approximately 630 Pa of water vapor for 60 minutes and then activated again at 175 °C for one hour. These samples were coded 25BEA-HH

and SZ-HH, respectively. Afterwards, all samples were exposed to approx. 650 Pa of pyridine vapor for 60 minutes at 100-150°C (zeolites) or 30 minutes at 150 °C (SZ). Physisorbed pyridine was allowed to desorb at the same temperature for 3 hours (zeolites) or 1 hour (SZ), and then total energy spectra were recorded at 25 °C. Reference spectra were obtained at 25 °C and 150 °C from KBr samples that were subjected to an in situ activation treatment similar to the corresponding catalyst samples. All heating and cooling rates were 10 °C/min. Total energy spectra were ratioed against the reference KBr spectra, and then the resulting reflectance spectra were converted with the Kubelka-Munk transformation. For the SZ and SZ-HH samples, the Lewis/Brönsted acidity ratio was calculated using the L/B extinction coefficient ratio and method suggested in [13]. No Brönsted acidity was detected in 75BEA, 25BEA or 25BEA-HH.

*2.4. Catalytic activity measurements*

Hydride transfer activities were measured on these materials using the test reaction between cyclohexene and isobutane at 80 °C. Cycloalkane products were counted as products of HT and DHGT. HT-only activities were determined by subtracting the cycloalkane amounts produced in the presence and in the absence of isobutane. Experimental details about the method are provided elsewhere [6].

In order to estimate the catalytic activity for alkylation, samples from each material, containing the fixed amount of 0.093 mmol acid sites (as measured by ammonia chemisorption), were first activated in an inert flow following the procedure described above, in the PFR reactor setup. Following activation and cooling to room temperature under the inert flow, the catalyst samples were quickly transferred into a stainless steel wire mesh basket inside a bench-top, stirred and temperature-controlled reactor (Parr model no. 4565, 100 $cm^3$, 316 stainless steel). Some of the SZ and 25BEA65 catalyst samples were exposed for one hour to approx. 630 Pa of water vapor in an attempt to modify their Lewis/Brönsted acid ratio, prior to being transferred into the reactor.

These samples were coded SZ-HH and 25BEA65-HH, respectively. Following loading into the reactor, all catalyst samples were evacuated for about one hour, after which a flow of 50 sccm of UHP helium was established through the reactor. A second, in situ activation was performed at 175 °C for one hour to remove physisorbed water acquired during catalyst loading. Samples that were pre-exposed to water vapor as described above were also subjected to this activation step in order to remove excess physisorbed water. Following the in situ activation, the reactor was cooled and held at a temperature of 80 °C, evacuated, and then refilled with isobutane (Matheson, 99%) vapor directly from the tank up to 3.46 bar. Separately and similarly, a 10-cc syringe was filled with 1-butene (Matheson, 99%) vapor up to 2.97 bar. The butene was mixed in four syringe washes with isobutane from and back into the reactor through heated tubing and fittings, in order to improve the transfer of the butene. Two subsequent washes were done with UHP argon at 3.76 bar into the reactor. The total elapsed time for butene introduction into the reactor was less than 2 minutes. Separate, blank tests showed that in average about 52% from the theoretical amount of butene was transferred into the reactor, and that the initial isobutane/butene ratio was between 15 and 25. The reactor was operated in a batch, gas phase mode. Samples were taken starting as early as 5 minutes on-stream, every 30 minutes, for a few hours. A typical initial pressure following the butene injection was 4.03–4.45 bar, with a pressure loss of about 0.14–0.34 bar per each sample. The samples were extracted using a heated needle valve and sent for analysis through the online sampling loop of a mass spectrometer-coupled gas chromatograph (Hewlett-Packard model GCD G1800A) equipped with a 30-m Supelco Supel-Q-Plot capillary column. $C_8$-range saturates included 2,2,4-trimethylpentane (TMP) and dimethylhexane (DMH) isomers. Separation of the individual DMHs was not achieved, and neither was the separation of individual $C_8$-range alkenes ($C_8^=$). Instead, each of these groups was lumped. Separation between the DMHs and $C_8^=$ groups was enhanced by extracting the specific ion fragment signals 57 and 43, respectively. In the calculation of conversions, the observed *cis*- and *trans*-butenes were counted

towards unreacted butene, while in the estimation of cracking activity, the n-pentane concentration was recorded.

## 3. Results and discussion

### *3.1. Characterization results*

Table 1 summarizes all the measured characteristics for the four materials tested. Surface acid site density and adsorbed isobutane/acid site ratios have been calculated in order facilitate the interpretation of the reaction results. Considering the 65% zeolite concentration in the 25BEA65 and 75BEA65 materials, the measured ammonia chemisorption values are in agreement with reported values obtained from ammonia temperature-programmed desorption measurements [5,14,15]. The availabilities for hydride transfer (AHT) are a measure of HT activity and are determined from the number of moles of HT products formed per each mole of acid during the test reaction of cyclohexene with isobutane [6]. The AHT values are shown as differences between tests in the presence and in the absence of isobutane, and therefore are not affected by dimerization/hydrogen transfer (DGHT). The higher AHT in the 25BEA65 material as compared to 75BEA65 is in accord with previous theoretical calculations [16] showing that a higher density of aluminum sites in a zeolite promotes HT by stabilizing intermediates formed during HT. Although of a much higher acid density than any of the zeolites, the low HT activity of SZ was explained by its much lower isobutane adsorption capacity, while in zeolite 80ZSM565, HT was blocked sterically by the narrower pore structure.

### *3.2. Alkylation tests*

The batch alkylation test results in Figure 1 are represented as productivities by normalizing the produced amounts of 2,2,4-trimethylpentane (TMP), the total dimethylhexanes (DMH) and the

total $C_8$ alkenes ($C_8^=$), to the number of acid sites that were measured by ammonia chemisorption. Most butene conversion was achieved within the first 5 minutes of reaction on all materials with the maximum apparent conversion being recorded on 75BEA65. The apparent butene conversion on this material continued to increase over the first 50 minutes before stabilizing, whereas conversion was observed to decrease and reach a minimum on all other materials. In all cases unreacted butene was almost completely isomerized to *cis*- and *trans*-butene. At the same time, the production of both $C_8^=$ and DMH steadily increased for all materials while a steady TMP concentration was reached within minutes for all catalysts except 80ZSM565. These observations indicate that on all catalysts (except 80ZSM565) sites active for TMP production deactivate rapidly, while dimerization is still possible on the remaining, possibly weaker active sites, as indicated by the evolution of $C_8^=$ and DMH [17]. The apparent *drop* in butene conversion with reaction time on 25BEA65, SZ and 80ZSM565 is attributed to the gradual reactor depressurization with each sample and the subsequent release of isomerized butene from the weakest acid sites. The observed increase in butene conversion with the 75BEA65 catalyst could be due to the accumulation of heavier oligomers from butene adsorbed on its stronger sites, or perhaps to a slow rate of butene adsorption. Compared to 25BEA65, the less dense acid sites in this material would allow oligomeric intermediates to build up to a greater extent before any hydride transfer or cracking on an adjacent site could proceed.

### *3.3. Effect of measured hydride transfer activity*

TMP is primarily a product of HT in the sequence of reactions 1 through 3. Indeed, 25BEA65, which showed the highest AHT value in the reaction of cyclohexene with isobutane, also had the highest TMP productivity. Moreover, zeolite ZSM-5 for which no AHT was detected, but which had significant DHGT activity [6], did not produce any saturates. Yoo and Smirniotis [5] have found that in a series of Beta zeolites of different SAR values, maximum 2-butene conversion for liquid-phase alkylation at 80 °C was obtained for SAR values between 17 and 30. While little

detail regarding the variation of the alkylate yield with SAR was given, the cited result is somewhat consistent with the finding here that the higher aluminum content enhances alkylation activity. A relatively good correlation exists between the AHT values and the observed TMP productivities, as shown in Figure 2. This finding directly confirms that HT, as opposed to DHGT, is the key factor in the production of TMP for all the materials analyzed. However, noticeable deviations can be observed in this correlation. In the case of 75BEA65, a lower than expected TMP productivity was recorded. As indicated by the observed increase with reaction time in butene conversion in Figure 1, a steady accumulation of butene keeps occurring with a slightly lower $C_8^=$ release rate than in the other materials. Thus, a slightly deeper oligomerization of adsorbed butene could have contributed to an early pore blockage, limiting the availability of active sites for HT reactions. It is likely that such a process was limited in the HT test reaction with cyclohexene because cyclohexene oligomer intermediates are bulkier and could easily have been size-restricted in the narrow zeolite pores.

On the other hand, SZ showed a slightly higher TMP production than expected from the AHT values and at the same time had the highest rate of $C_8^=$ formation. This slight enhancement in TMP could be the effect of early oligomerization, subsequent cracking and hydrogen transfer, as suggested by Corma et al [17]. Indeed, when comparing the relative amounts of n-pentane produced by the four materials up to 130 min reaction time, the following series is found: SZ (5.0) > 25BEA65 (1.5) > 75BEA65 (1.0) > 80ZSM565 (0.0). The very high acid site density (Table 1) and strength in this material are most probably responsible for the higher oligomerization and cracking rates during alkylation, whereas cyclohexene oligomers are expected to be resistant to cracking in the HT test reaction.

*3.4. Effect of moisture*

Because previous investigations have suggested that Brönsted acidity is necessary for alkylation [3], an attempt was made to modify the two most active catalysts 25BEA65 and SZ by water vapor exposure (resulting materials coded 25BEA65-HH and SZ-HH). The alkylation results for these catalysts are compared to those for the "dry" catalysts in Figure 3. Following the in situ reactivation of these materials at 175 °C, both suffered a significant decrease in the quantities of TMP and DMH produced, while their $C_8^=$ productivities remained virtually unchanged. An interesting effect was observed in the butene conversion trends where SZ-HH converted more butene than the corresponding, "dry" SZ. In both materials that were exposed to water vapor, cracking activity did not significantly change (as indicated by n-pentane formation) but TMP and DMH formation was inhibited. However, n-pentane is also a saturated hydrocarbon formed by HT and/or DHGT from the corresponding carbocation intermediate. Therefore, water exposure seemed to selectively inhibit the HT reactions that yield $C_8$ saturates without significantly affecting other reactions. The 25BEA-HH and SZ-HH materials were tested using the IR spectroscopy of chemisorbed pyridine in the DRIFTS apparatus with the purpose of measuring any change in the relative Lewis/Brönsted (L/B) acidity. After in situ reactivation at 175 °C, no significant change in the L/B ratio was detected for SZ-HH. An approximate L/B value of 1.1 was measured both in the freshly activated SZ [13] and in SZ-HH. However, neither 25BEA nor 25BEA-HH showed any Brönsted acidity, following the *in-situ* activation in the DRIFTS accessory. In fact, the 75BEA catalyst also lacked Brönsted acidity. This lack of Brönsted acidity was attributed to the activation of the zeolites in a completely dry atmosphere at 500 °C and TGA/MS measurements confirmed that a structural water loss occurred at about 450-500 °C. This is in accord with earlier findings [18] that activation at increasing temperatures in dry inert flows leads to successively lower Brönsted acidity in Beta zeolites. Although the studied Beta zeolites completely lacked Brönsted acidity in the DRIFTS apparatus, they were active for both HT and alkylation. Because of the high-temperature activation of the zeolites, the separate influence of

Brönsted acidity, if any, could not be evaluated. On the other hand, the decrease in $C_8$ saturate selectivity in 25BEA65-HH and SZ-HH when compared to25BEA65 and SZ shows that a certain modification was induced in the catalysts by water exposure. If the reactivation for one hour at 175 °C only partially removed physisorbed water, competitive physisorption between water and isobutane produced a lower adsorbed isobutane/acid site ratio than the values shown in Table 1. In SZ-HH on the other hand, the increase in butene conversion could be due to a slight change in the L/B ratio under the effect of adsorbed water, which might have been below the sensitivity limit of the DRIFTS method. It was previously shown that a fast Lewis-Brönsted interconversion is possible in sulfated zirconia (see for ex. [13,19]). Thus, the change in SZ-HH surface chemistry caused by the creation of a small number of new Brönsted acid sites could have accounted for the increased butene conversion.

*3.5. Effect of catalyst interaction with reactants*

The catalyst loadings in the alkylation batch experiments were such that a constant 1-butene/acid molar ratio of about 6.3 was used in each experiment. In Figure 1, the drop in the apparent butene conversion with advancing sample number—and inherent pressure drop in the reactor—seems to indicate that some butene is reversibly adsorbed on all catalysts except 75BEA65. At the same time, all catalysts showed relatively similar $C_8^=$ productivities per acid site regardless of the different butene conversions observed. As evidenced in Figure 4, a correlation can be established between the total catalyst surface area and butene conversion. This correlation promptly indicates that the observed "conversion" is a strong function of the adsorption capacity of the catalyst. Separate volumetric butene adsorption experiments showed that on all catalysts equilibrium could not be reached even after 48 h, so that butene total adsorption measurements were not usable. Whether this steady butene accumulation was by reversible physisorption or by irreversible chemisorption remains unclear. However, during isobutane adsorption experiments equilibrium was reached relatively fast on all materials and no

chemisorption could be detected. Therefore, the overall interaction (physical and chemical) between the solid acids studied and isobutane is weaker than with butene. If the productivity of $C_8$ alkenes per acid site is thought of as an indication of the extent of butene oligomerization, it can be concluded from Figure 1c that, except on the narrower-pore 80ZSM565, oligomerization is only a function of the number of acid sites available and is not affected by the apparent butene conversion. It could therefore be argued that at least under the studied experimental conditions, competitive adsorption favoring butene to isobutane is partially lowering the alkylate production by blocking the access of isobutane to the active sites and is at the same time responsible for a fraction of the apparent butene conversion. Judging by these observations, the negative deviation in the TMP – AHT correlation in Figure 2 corresponding to 75BEA65, and the positive deviation observed for SZ, could be seen as a result of competitive adsorption.

## 4. Conclusions

Batch isobutane alkylation tests with 1-butene performed under gas-phase conditions have shown a good correlation between the amount of TMP produced per acid site and the independently measured low-temperature HT activity. Under the current conditions, alkene formation was favored. The lack of any alkylation activity in the ZSM-5 catalyst correlated perfectly with its complete lack of HT activity even though it had an elevated DHGT activity. Sites initially active for alkylation deactivate rapidly, while the remaining sites maintain oligomerization activity, as evidenced by $C_8^=$ and DMH evolution. On the basis of the test reaction between cyclohexene and isobutane, SZ showed a higher than expected productivity of TMP, attributable to intense oligomerization and cracking, while 75BEA65 showed lower than expected yields of $C_8$ due to advanced oligomerization. 25BEA65 had the highest low-temperature HT activity and produced the most TMP in the alkylation tests.

No Brönsted acidity was detected in the 25BEA and 75BEA catalyst samples that were activated in the DRIFTS apparatus at 500 °C in a completely dry inert. Exposure of 25BEA65 and SZ to water vapor at room temperature did not create any new Brönsted sites, however this treatment selectively inhibited their alkylation activity with no change in $C_8$ alkene formation. It is therefore desirable that moisture not be present in any of these catalysts in order to achieve higher alkylation selectivities. In the water-exposed SZ, an increased butene conversion was detected compared to the dry catalyst and could be explained by changes in the surface chemistry below the sensitivity of the DRIFTS method.

Finally, the observed butene conversion correlated with the total surface area exposed by the catalysts to the reaction mixture, indicating that this conversion was due in part to reversible adsorption of butene on the weakest acid sites. Evidence indicates that all the studied catalysts adsorbed butene stronger than isobutane. While isobutane chemisorption was not observed on any of the catalysts, 1-butene was strongly adsorbed and equilibrium adsorption was not achieved, even after 48 hours. It was concluded that a partial cause of limited alkylation activity under the reaction conditions studied could be the competitive adsorption that favors butene versus isobutane, thus lowering the access of the hydride donor to the active sites. An increase of the isobutane availability for the HT step (such as an increase in the isobutane adsorption capacity) at the expense of butene adsorption is thought to be necessary in order to promote alkylation reactions.

*Acknowledgements*

This work was carried on in, and funded through the O.H. Reaugh Laboratory for Oil and Gas Processing Research at Washington State University.

*References*


[1] S.I. Hommeltoft, Appl. Catal. A 221 (2001) 421.

[2] J.M. Meister, S.M. Black, B.S. Muldoon, D.H. Wei, C.M. Roesler, Hydrocarbon Processing 79 (2000).

[3] A. Feller, I. Zuazo, A. Guzman, J.O. Barth, J.A. Lercher, J. Catal. 216 (2003) 313.

[4] D.B. Lukyanov, J. Catal. 145 (1994) 54

[5] K. Yoo, P.G. Smirniotis, Appl. Catal. A 227 (2002) 171

[6] A. Platon, W.J. Thomson, in preparation

[7] A. Corma, P.J. Miguel, A.V. Orchillés, Appl. Catal. A 138 (1996) 57

[8] K. Hatakeyama, T. Suzuka, M. Yamane, Sekiyu Gakkaishi 34 (1991) 267

[9] A. Corma, M.I. Juan-Rajadell, J.M. Lopez-Nieto, A. Martinez, C. Martinez, Appl. Catal. A 111 (1994) 175

[10] Y.F. Chu, A.W. Chester, Zeolites 6 (1986) 195

[11] R. B. Gore, W. J. Thomson, Appl. Catal. A 168 (1998) 23

[12] A.S. Chellappa, R.C. Miller and W.J. Thomson, Appl. Catal. A 209 (2001) 359

[13] A. Platon, W.J. Thomson, Ind. Eng. Chem. Res. 42 (2003) 5988

[14] G.S. Nivarthy, K. Seshan, J.A. Lercher, Microporous Mesoporous Mater. 22 (1998) 379

[15] G.S. Nivarthy, Y. He, K. Seshan, J.A. Lercher J. Catal. 176 (1998) 192

[16] C.J.A. Mota, P.M. Esteves, M.B. de Amorim, J. Phys. Chem., 100 (1996) 12418

[17] A. Corma, A. Martinez, C. Martinez, J. Catal. 149 (1994) 52

[18] E. Baburek, J. Novakova, Appl. Catal. A 185 (1999) 123

[19] B. Li, R.D. Gonzalez, Catal. Today 46 (1998) 55.

Table 1. Measured and calculated characteristics of the catalysts used in the study. (S.A. – surface area, $iC_4$ – isobutane, AHT – site availability to HT)

| | dry weight | | BET S.A. | $NH_3$ chemisorption | | | $iC_4$ total adsorption | | | AHT |
|---|---|---|---|---|---|---|---|---|---|---|
| material | wt% | ± % | $m^2$/g(dry) | mmol/g | ± % | μmol/$m^2$ | mmol/g(dry) | ± % | $iC_4$:acid | mol/mol acid |
| 75BEA65 | 91.9 | 0.19 | 441 | 0.254 | 7.5 | 0.58 | 0.733 | 0.8 | 2.89 | 0.065 |
| 25BEA65 | 90.5 | 0.01 | 444 | 0.572 | 1.3 | 1.29 | 0.780 | 0.0 | 1.36 | 0.073 |
| SZ | 97.4 | 0.11 | 90 | 0.230 | 1.7 | 2.56 | 0.034 | 10.0 | 0.15 | 0.029 |
| 80ZSM565 | 95.7 | 0.07 | 333 | 0.336 | 5.5 | 1.01 | 0.377 | 1.8 | 1.12 | - |

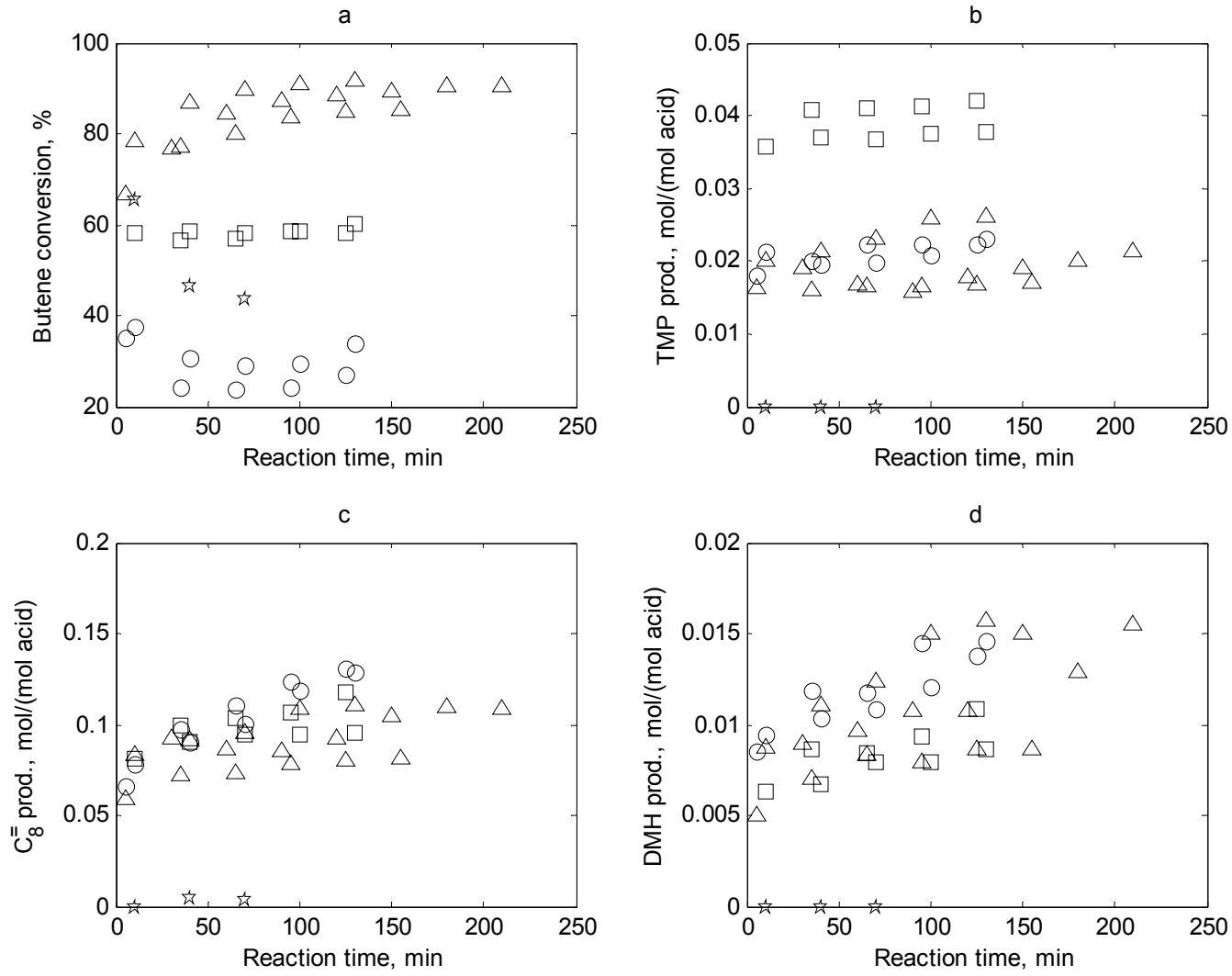


Figure 1. Batch alkylation results: a – butene conversion (*cis*- and *trans*-butene all accounted for unreacted butene); b – 2,2,4-trimethylpentane productivity; c – total $C_8$-range alkene productivity; d – dimethylhexane productivity. Symbols represent: △ – 75BEA65 (3 experiments); □ – 25BEA65 (2 experiments); ○ – SZ (2 experiments); ☆ – 80ZSM565.

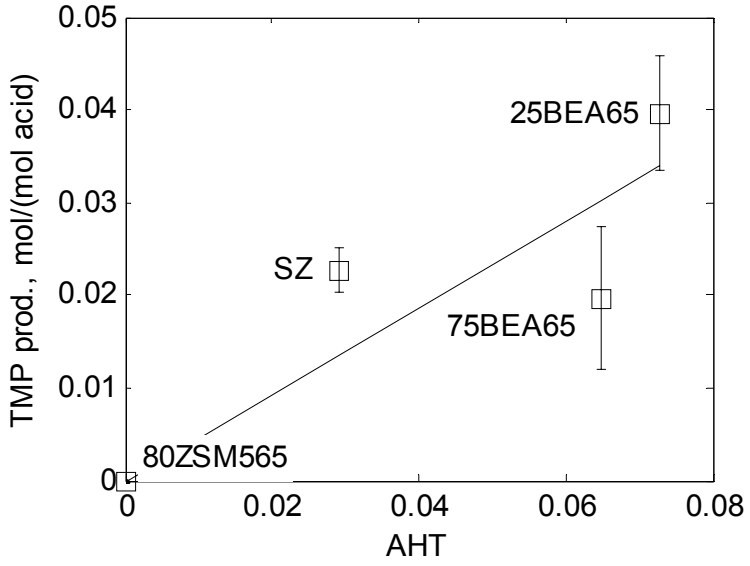


Figure 2. Correlation of TMP productivity during the alkylation test with the apparent acid site availability for hydride transfer (AHT) as measured with the cyclohexene+isobutane test reaction. (TMP values are estimated from linear regression at 130 min reaction time; error bars calculated for 95% confidence)

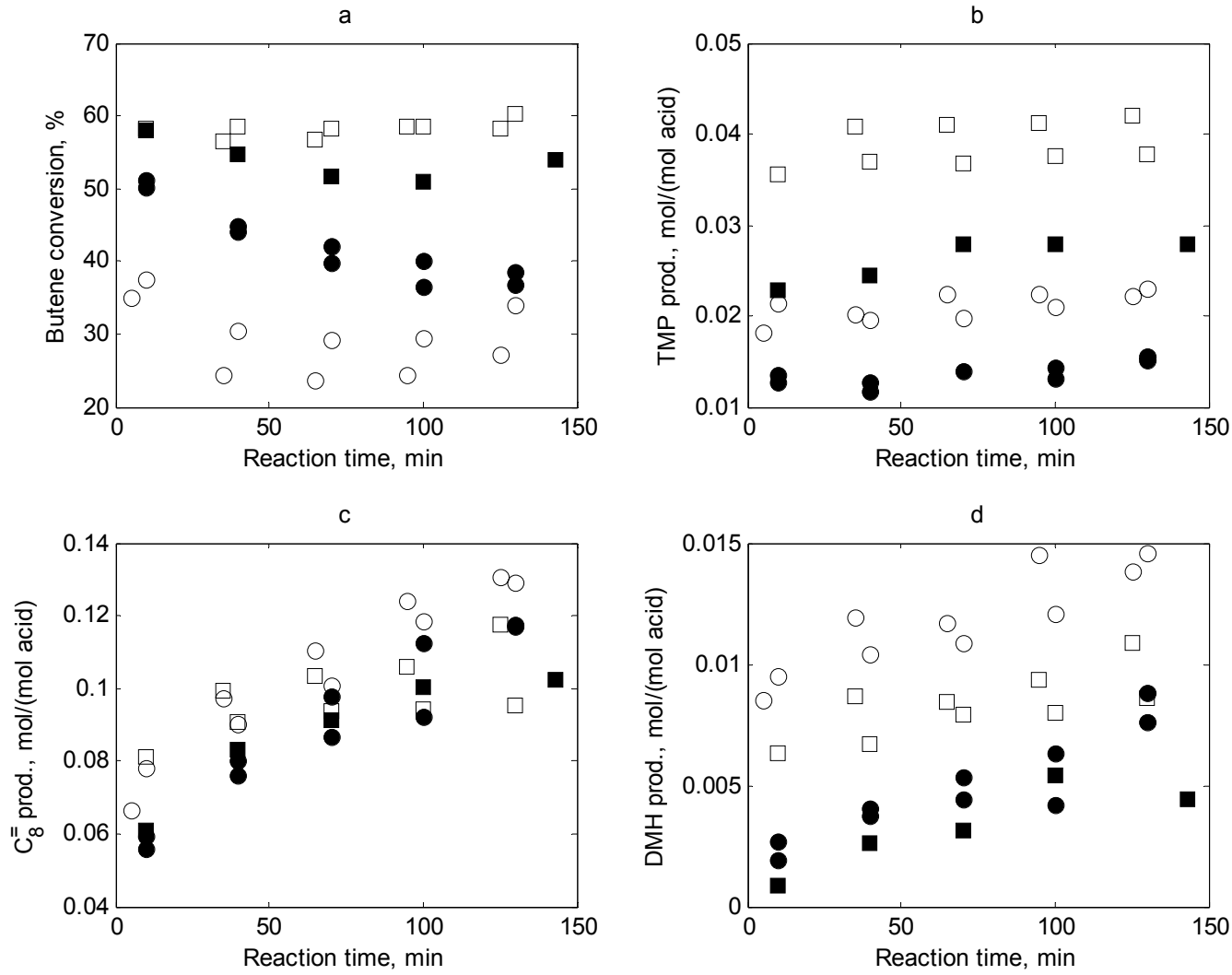


Figure 3. Effect of water pre-exposure upon batch alkylation results: a – butene conversion (*cis*- and *trans*-butene all accounted for unreacted butene); b – 2,2,4-trimethylpentane productivity; c – total $C_8$-range alkene productivity; d – dimethylhexane productivity. Symbols represent: □ – 25BEA65 (2 experiments); ■ – 25BEA65-HH; ○ – SZ (2 experiments); ● – SZ-HH (2 experiments).

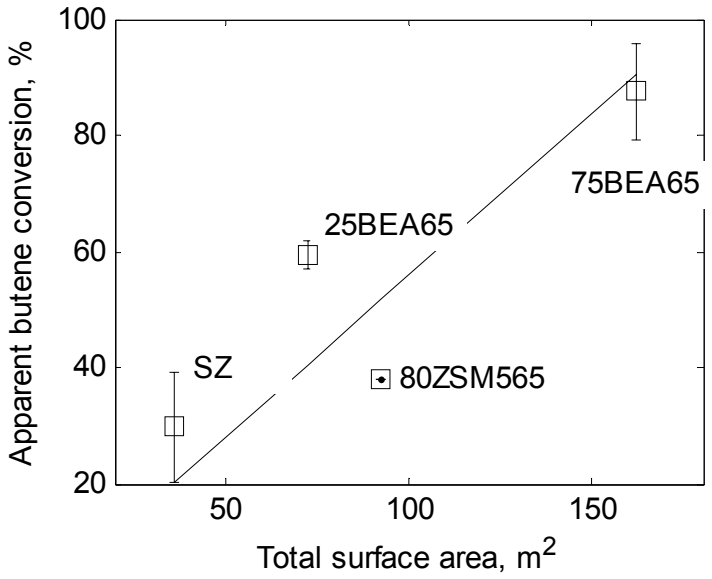


Figure 4. Correlation between the total catalyst surface area and the observed butene conversion during the alkylation tests. 2-Butenes (*cis* and *trans*) were considered unreacted butene. (conversion values are estimated from linear regression at 130 min reaction time; error bars calculated for 95% confidence)

# APPENDIX A

## PYRIDINE/DRIFTS MEASUREMENTS AND DATA

Spectra of pyridine interacting with sulfated zirconia were collected as total energy spectra and thereafter ratioed against total energy spectra obtained from KBr samples. Specific peaks corresponding to the Bpy and Lpy species were integrated numerically on the intervals 1565–1510 $cm^{-1}$ and 1465–1424 $cm^{-1}$. It was shown before that the slope of a Lpy–Bpy plot is the negative of the ECR. Variability is possible in powder packing affecting the scattering factor and the optical density of the samples, however, the slope of the Lpy–Bpy plot should, at least in theory, hold constant from one sample to another. Errors introduced by such factors as inconsistent catalyst activation/dehydration, or inconsistent desiccation of pyridine or inert gas should be this way eliminated provided the linearity of the Kubelka-Munk transform with concentration holds, and chemisorbed pyridine is not displaced by water exposure. In practice however, the major source of experimental error came from variable water vapor interference along the optical path of the FTIR instrument. It was not uncommon to detect in the acquired data changes in outside precipitation, or the presence or absence of laboratory coworkers. The data acquired (Table A1, Figure A1) showed a significant number of outliers that were most probably related to variations in ambient humidity.

The raw ECR data from Table 1 was plotted in Figures A1(A) and (B) as a run sequence plot and a lag plot. The run sequence plot is useful in revealing trends in data evolution (such as a slow drift in equipment sensitivity) as well as abnormal data (outliers). The lag plot is useful in pointing out both outliers and oscillations in equipment response (data “running in circles”). Some statistics on the raw ECR data are listed below:

Mean: 2.219476

Median: 0.2060000E+01

Standard deviation: 0.6887106

Standard deviation of mean: 0.1502890

95% confidence interval for actual mean: 1.90598 through 2.53297

A quick look at the run sequence plot shows that data tends to concentrate around the ECR value of 2.0. Looking at the fluctuations and jumps in the ECR values, there is no reason to trust data that fall outside the interval 1.5–2.5. Also the lag plot clearly shows about 6 outliers, and no significant oscillation. The outliers were eliminated from the calculation, and the resulting plots are shown in Figures A(C) and (D). The statistics on this filtered data are listed below. Noticeable is the coincidence between the new mean, median and the median from the raw, unfiltered data:

Mean: 2.049333

Median: 0.2050000e+01

Standard deviation: 0.2406677

Standard deviation of mean: 0.6214014E-01

95% confidence interval for actual Mean: 1.91606 through 2.18261

This ECR value was used to calculate the L/B ratio on the remaining data. The statistics for this data are listed below. The run sequence and lag plots in Figure A2 clearly show two outliers.

Mean: 1.106933

Median: 0.1088000E+01

Standard deviation: 0.2253494

Standard deviation of mean: 0.5818497e-01

95% confidence interval for actual Mean: 0.982139 through 1.23173

After the elimination of the two outliers, the updated statistical calculation shows a good match between the median and the mean L/B values:

Mean: 1.086385

Median: 0.1088000E+01

Standard deviation: 0.9894573E-01

Standard deviation of mean: 0.2744261E-01

95% confidence interval for actual Mean: 1.02659 through 1.14618

Table A1. Raw pyridine/DRIFTS data showing Lpy, Bpy peak areas before and after hydration as well as the calculated ECR values.

| Expt | Sample | Peak Limits, $cm^{-1}$ | Initial Bpy area | Initial Lpy area | Final Bpy area | Final Lpy area | ECR |
|---|---|---|---|---|---|---|---|
| 20020930 | SZ | 1565-1510 1465-1424 | 4.099 | 14.870 | 7.631 | 9.340 | 1.566 |
| 20021001 | SZ | 1565-1510 1465-1424 | 5.954 | 13.245 | 9.494 | 6.486 | 1.909 |
| 20021002 | SZ | 1565-1510 1465-1424 | 5.337 | 13.009 | 9.026 | 6.328 | 1.811 |
| 20021007 | SZ | 1565-1510 1465-1424 | 5.962 | 13.327 | 9.551 | 4.481 | 2.464 |
| 20021008 | SZ | 1565-1510 1465-1424 | 5.297 | 13.434 | 8.064 | 5.414 | 2.898 |
| 20021014 | SZ | 1565-1510 1465-1424 | 5.854 | 11.482 | 8.860 | 2.760 | 2.902 |
| 20021016 | SZ | 1565-1510 1465-1424 | 6.004 | 13.484 | 10.397 | 4.772 | 1.983 |
| 20021017 | SZ | 1565-1510 1465-1425 | 5.093 | 12.907 | 8.824 | 5.367 | 2.021 |
| 20021018 | SZ | 1565-1510 1465-1426 | 5.597 | 13.435 | 9.457 | 5.509 | 2.054 |
| 20021108 | SZ | 1565-1510 1465-1427 | 6.622 | 11.749 | 10.165 | 4.453 | 2.060 |
| 20021112 | SZ | 1565-1510 1465-1428 | 6.837 | 13.509 | 10.560 | 4.530 | 2.411 |
| 20021113 | SZ | 1565-1510 1465-1429 | 5.744 | 12.603 | 9.514 | 4.356 | 2.187 |
| 20021115 | SZ | 1565-1510 1465-1430 | 5.642 | 12.253 | 9.817 | 4.935 | 1.753 |
| 20021118 | SZ | 1565-1510 1465-1431 | 5.142 | 12.453 | 9.067 | 3.519 | 2.276 |
| 20021120 | SZ | 1565-1510 1465-1432 | 4.981 | 10.517 | 8.590 | 2.497 | 2.222 |
| 20030305 | SZ | 1565-1510 1465-1424 | 4.813 | 11.070 | 7.926 | 4.597 | 2.079 |
| 20021122 | 10%SZ/KBr | 1565-1510 1465-1433 | 0.313 | 0.593 | 0.730 | 0.086 | 1.218 |
| 20021127 | 10%SZ/KBr | 1565-1510 1465-1434 | 1.493 | 2.064 | 2.144 | 0.227 | 2.824 |
| 20021202 | 10%SZ/KBr | 1565-1510 1465-1435 | 1.050 | 1.245 | 1.295 | 0.132 | 4.532 |
| 20021204 | 10%SZ/KBr | 1565-1510 1465-1436 | 0.291 | 0.532 | 0.576 | 0.124 | 1.430 |
| 20021206 | 10%SZ/KBr | 1565-1510 1465-1437 | 0.422 | 0.620 | 0.683 | 0.096 | 2.009 |

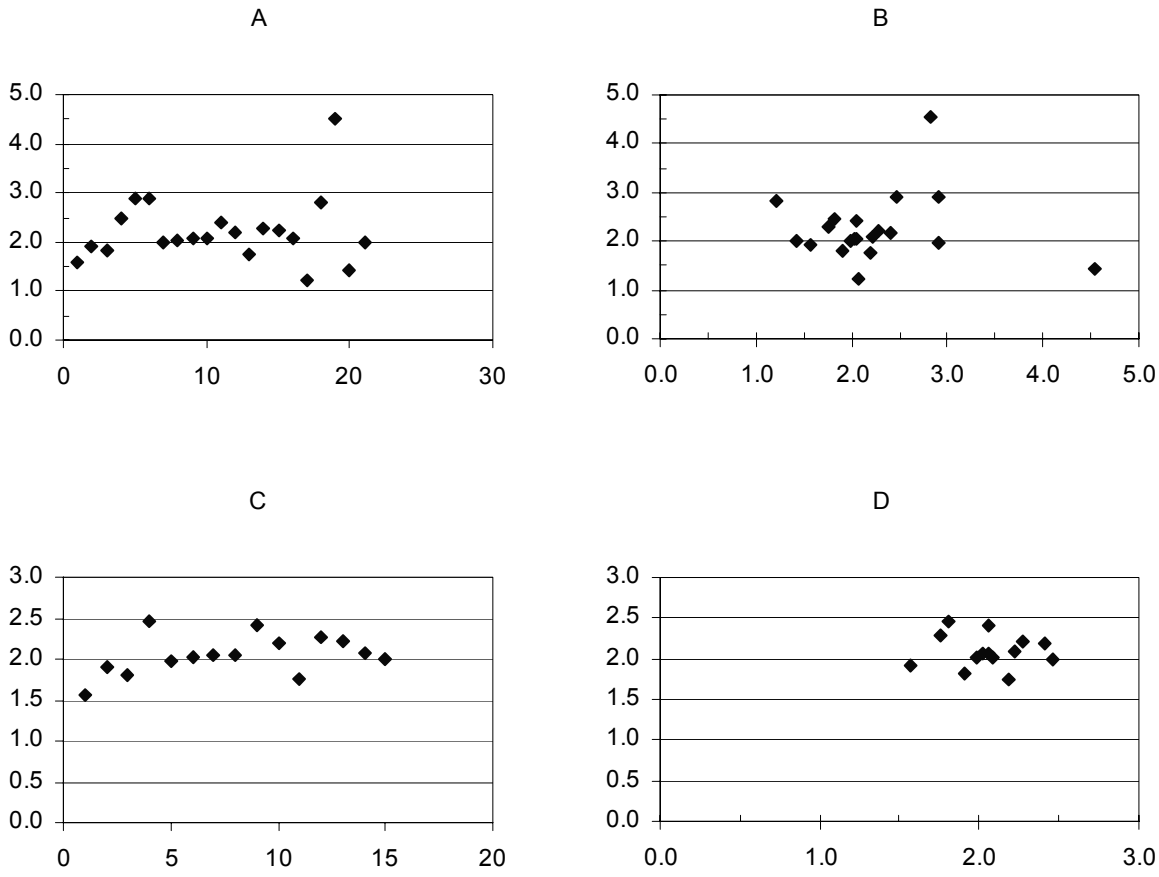


Figure A1. Run sequence plots (A, C) and lag plots (B, D) for the ECR data before (A, B) and after (C, D) the elimination of outliers.

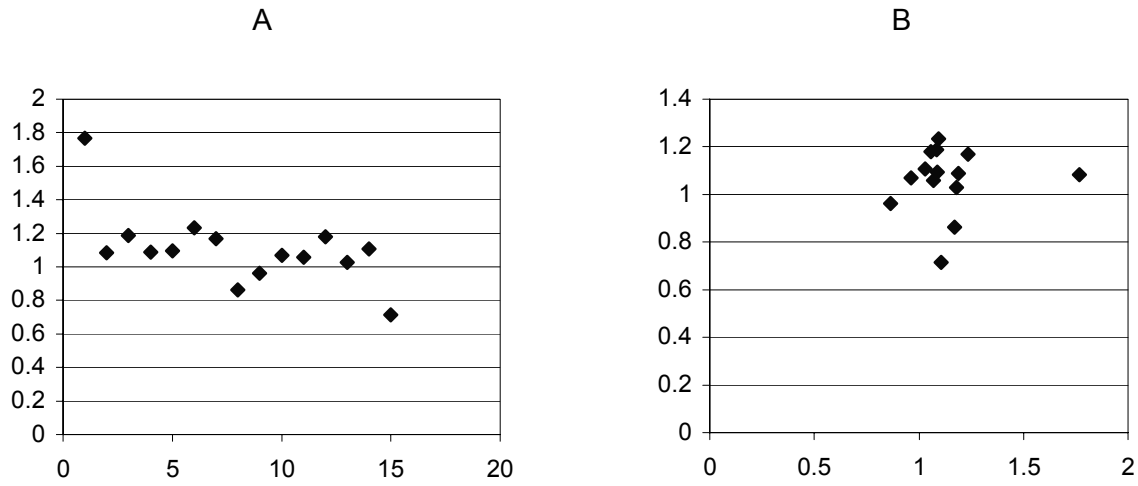


Figure A2. Run sequence plot (A) and lag plot (B) for the L/B data before the removal of two outliers.

# APPENDIX B

## TGA/MS MEASUREMENTS AND DATA

As stated in Chapter Three, TGA/MS experiments were carried in order to (1) measure the catalyst dry weights that all subsequent chemisorption and adsorption capacities were normalized to, and (2) identify the optimal catalyst activation pretreatment that would be consistent from one catalyst sample to another. Two major constraints existed for the activation temperature of the zeolites materials: (1) zeolites 25BEA and 80ZSM5 were purchased in their ammonium form, and therefore, they required decomposition into the acidic form, and (2) the maximum temperature achievable with the hydride transfer test setup was 510 °C. Based on the decomposition profiles shown in Figures B1—B3, a common decomposition/activation temperature for all zeolite materials was selected to be 500 °C. In figure B4, the decomposition profiles for SZ show a major sulfate loss peak above ca. 700 °C, and therefore the dry weight was calculated only up to 650 °C. Also, based on the weight loss curve, an activation temperature of 350 °C was considered sufficient for this material.

All dry weight results are summarized in Table B1.

A

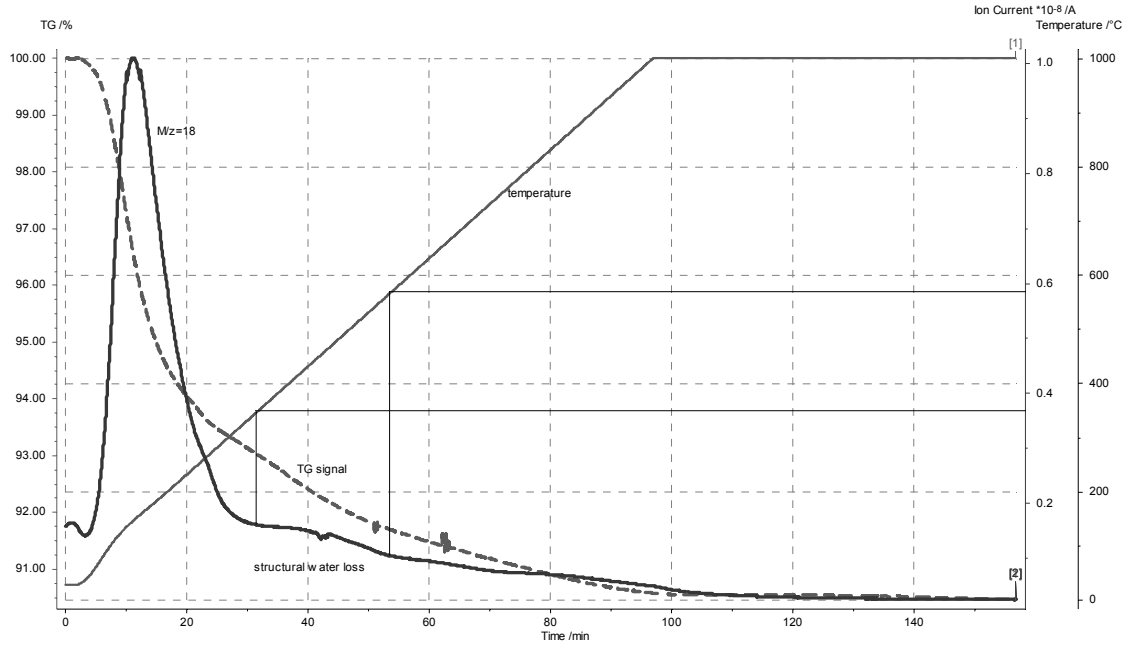


B

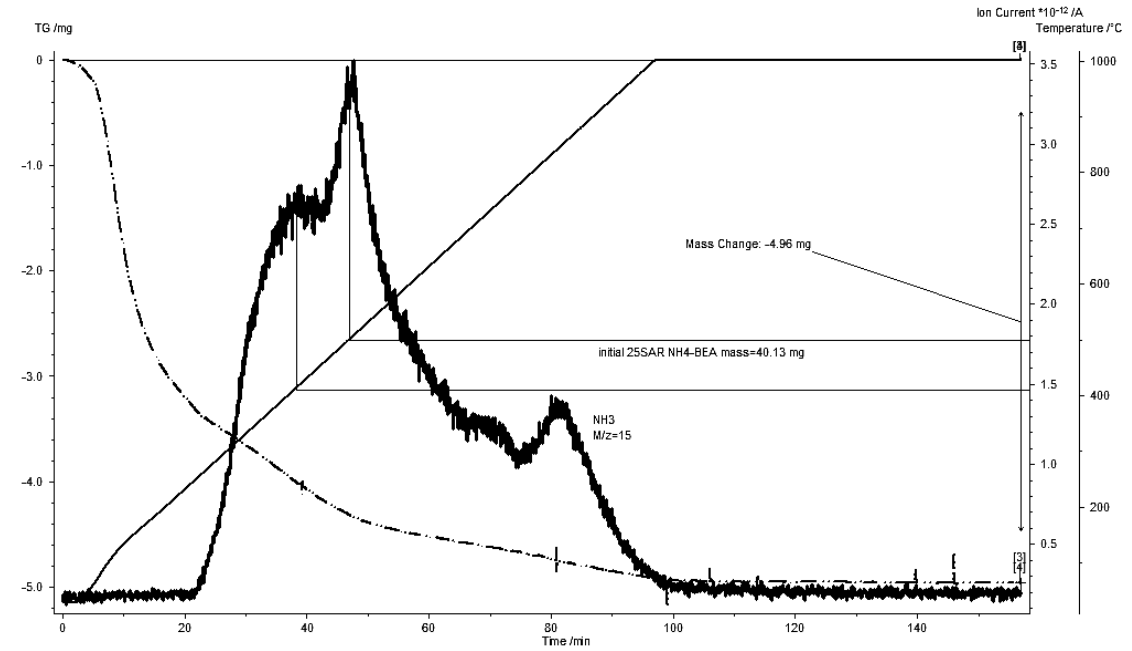


Figure B1. TGA/MS profiles for the decomposition/activation of 25BEA65. A – Data showing temperature ramp, relative weight and mass spectrometer fragment M/z=18 (mostly water); B – Data from a different experiment showing temperature ramp, relative weight and fragment M/z=15 (mostly ammonia) which peaks at ~400 °C, ~500 °C and ~850 °C.

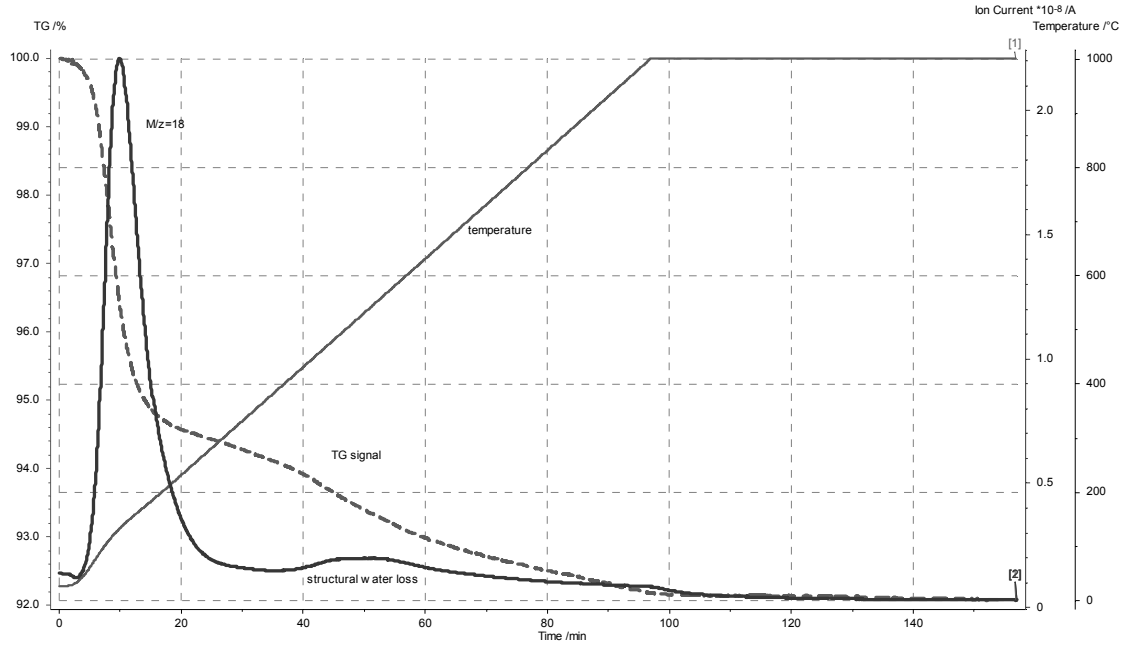


Figure B2. TGA/MS profiles for the activation of 75BEA65. Up to 500 °C, two important water losses (M/z=18) occurred, at ~180 °C and ~500 °C.

A

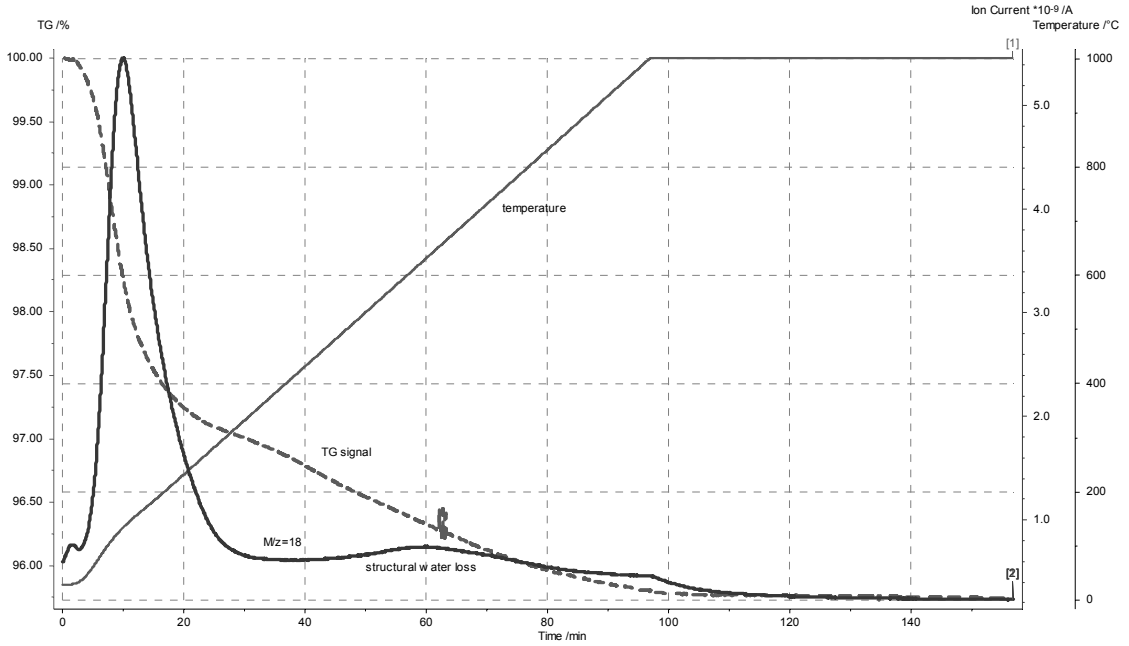


B

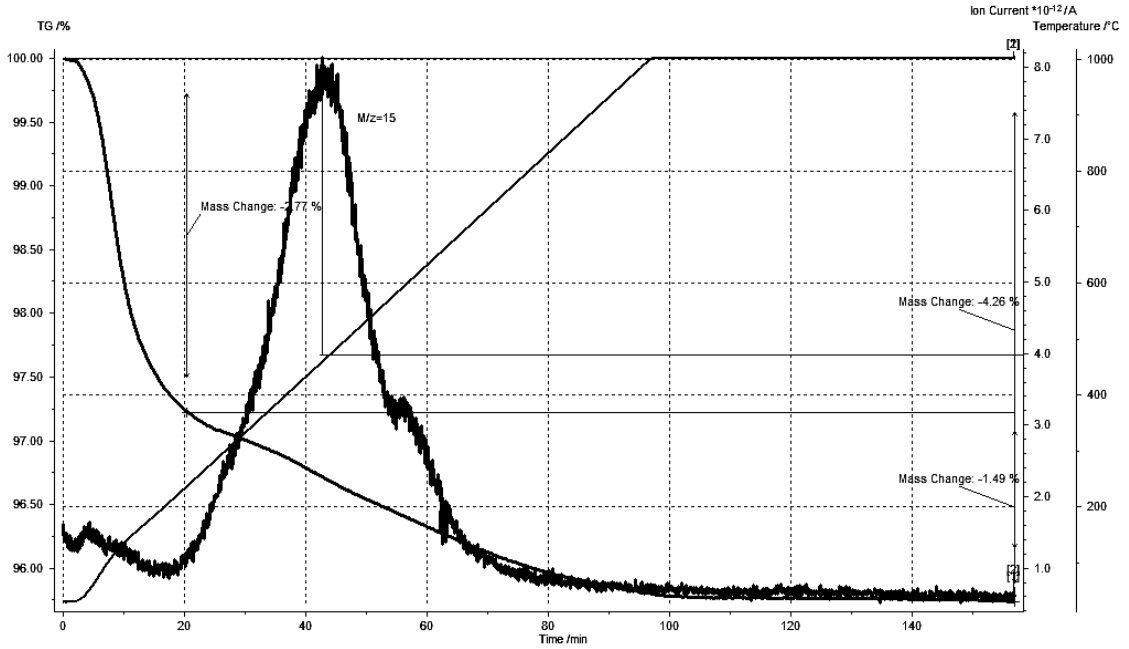


Figure B3. TGA/MS profiles for the activation/decomposition of 80ZSM565. A – Data showing temperature ramp, relative weight and fragment M/z=18 (mostly water); B – Data from the same experiment showing temperature ramp, relative weight and fragment M/z=15 (mostly ammonia) which peaks at ~480 °C

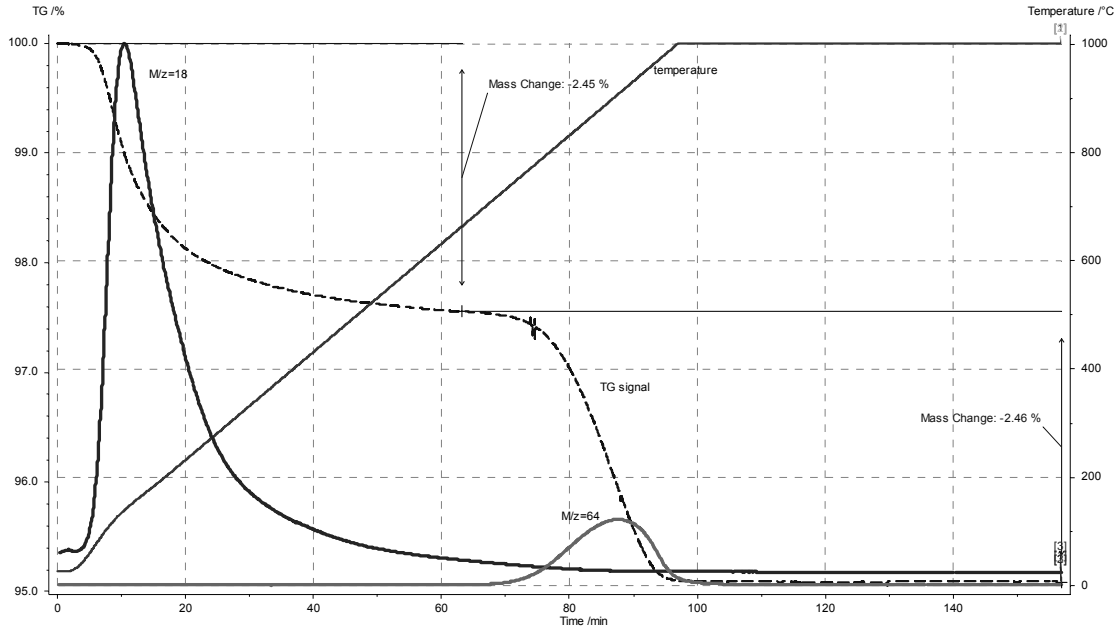


Figure B4. TGA/MS profiles for the activation of SZ. A major sulfur loss occurs above ~700 °C (M/z=64, $SO_2$), and the most important water loss occurs at ~110 °C.

Table B1. TGA/MS weight loss results

| | %wt. loss to 1000°C 10°C/min | | | | |
|---|---|---|---|---|---|
| material | Run #1 | Run #2 | Run #3 | average | ± % |
| 25NH4BEA65 | 9.55 | 9.54 | 9.56 | 9.55 | 0.1 |
| 75BEA65 | 7.93 | 8.11 | 8.23 | 8.09 | 2.1 |
| 80NH4ZSM565 | 4.26 | 4.36 | 4.36 | 4.33 | 1.5 |
| SZ* | 2.45 | 2.59 | 2.64 | 2.56 | 4.4 |

* Weight loss determined only up to 650 °C.

## APPENDIX C

## AMMONIA AND ISOBUTANE ADSORPTION – MEASUREMENTS AND DATA

Reactant adsorption and chemisorption measurements were carried out in the ASDI RXM-100 catalyst characterization apparatus. Catalyst samples were loaded in bulb-type reactors. Gases are expanded from a calibrated volume (reaction manifold, RMF, of volume 10.956 $cm^3$) into the reactor while pressures are precisely measured (±0.01 torr). Based on the typical reactor sizes used, the theoretical sensitivity with this method is about $5\times10^{-6}$ mmol. Much larger uncertainties, however, arise from the varying dry catalyst masses employed in the measurement, especially for highly hygroscopic materials such as SZ and all zeolites. Another source of experimental uncertainty is sample inhomogeneity. Especially in the case of silica-bound zeolites, variations in the measured (chemi)sorption values were correlated to some extent with the color shade of the catalyst particles, which were determined by the varying concentrations in zeolitic material.

For each catalyst, after the sample had been subjected to the activation treatments detailed in Chapter 3, a room-temperature expansion of ultra-pure helium was performed by putting the previously pressurized RMF in contact with the evacuated reactor and catalyst (Figure C1). The ratio between the final and initial pressure was recorded as the room-temperature expansion ratio, $E_0$:

$$E_0 = \frac{P_f}{P_i} = \frac{V_{RMF}}{V_{RMF} + V_{RA} + V_{RT}}$$

where: P – pressures: i – initial, f – final; $V_{RMF}$ – volume of reaction manifold (calibrated volume), $V_{RA}$ – equivalent reactor volume held at ambient temperature, $V_{RT}$ – equivalent reactor volume to be held at chemisorption temperature T.

The procedure was repeated with the reactor held at the desired (chemi)sorption temperature – in this case 80 °C, and the expansion ratio $E_T$ also recorded:

$$n = \text{constant} = \frac{P_i \cdot V_{RMF}}{R \cdot T_0} = P_f \cdot \left( \frac{V_{RT}}{R \cdot T} + \frac{V_{RMF} + V_{RA}}{R \cdot T_0} \right)$$

$$E_T = \frac{P_f}{P_i} = \frac{\frac{V_{RMF}}{T_0}}{\frac{V_{RT}}{T} + \frac{V_{RMF} + V_{RA}}{T_0}}$$

where: n – number of moles, $T_0$ – ambient temperature, T – temperature of catalyst sample, R – universal ideal gas constant.

From the above formulas, the volumes held at temperature T (80 °C) – $V_{RT}$ – and at ambient temperature – $V_A = V_{RA}+V_{RMF}$ – were calculated:

$$V_{RT} = V_{RMF} \cdot \frac{T \cdot (E_T - E_0)}{E_T \cdot E_0 \cdot (T - T_0)}$$

$$V_A = V_{RMF} \cdot \frac{T \cdot E_0 - E_T \cdot T_0}{E_T \cdot E_0 \cdot (T - T_0)}$$

Thereafter, following complete evacuation, expansion of known pressures of adsorbate (ammonia or isobutane) was performed. The recorded pressures from each expansion step were

compared with the ideal-gas expected final pressures, and the difference in mole numbers was accounted for as the adsorbed quantity from the specific gas.

$$\Delta n_a = n_i - n_f = \frac{P_i \cdot V_{RMF}}{R \cdot T_0} - P_f \cdot \left( \frac{V_A}{R \cdot T_0} + \frac{V_{RT}}{R \cdot T} \right)$$

where: $\Delta n_a$ – number of moles adsorbed, $n_i$ – initial number of moles in RMF, $n_f$ – final number of moles in the gas phase.

Incremental re-pressurizations of the RMF and subsequent expansions into the reactor were performed without intermediate evacuations, thus allowing for the adsorption isotherms to be measured. The number of moles adsorbed during incremental step *k* is calculated as:

$$\Delta n_a^{(k)} = n_i^{(k)} - n_f^{(k)} = \left[ \frac{P_i^{(k)} \cdot V_{RMF}}{R \cdot T_0} + P_f^{(k-1)} \cdot \left( \frac{V_{RT}}{R \cdot T} + \frac{V_{RA}}{R \cdot T_0} \right) \right] - \left[ P_f^{(k)} \cdot \left( \frac{V_A}{R \cdot T_0} + \frac{V_{RT}}{R \cdot T} \right) \right]$$

The adsorption isotherm was obtained by calculating the integral adsorbed moles normalized to the dry weight of the catalyst sample as a function of equilibrium (final) pressure per each increment. For the purpose of this work, isotherm acquisition was considered completed once a linear, monolayer region was attained. In the cases where chemisorption occurred—such as with ammonia— the first adsorption isotherm included both physisorbed and chemisorbed adsorbate. Following an overnight evacuation at constant temperature it was considered that all physisorbed gas was removed. A similar, second adsorption measurement on the evacuated material was used to measure the physisorption isotherm. By subtracting the two isotherms in the linear, and parallel segments, the numbers of moles of chemisorbed adsorbate per gram of dry catalyst were calculated. A typical chemisorption data sheet is shown in Figure C2. The complete ammonia chemisorption data acquired are listed in Table C1.

In the case of isobutane used as an adsorbate, no chemisorption could be measured. The physisorption capacity of all catalysts was calculated by extrapolation of the adsorbed number of moles from the linear, monolayer isotherm to a zero pressure. The complete isobutane adsorption capacities measured are listed in Table C2.

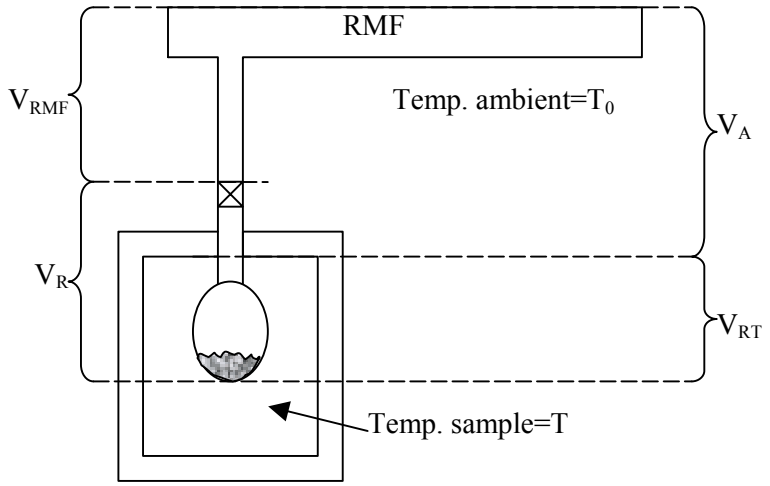


Figure C1. Volumetric measurement of ammonia chemisorption – derivation of calculation formulas.

Figure C2. Typical chemisorption data sheet.

| Date: | 040223 - 040226 | | | | Run: | NH3 chemisorption at 80 C | | | | |
|---|---|---|---|---|---|---|---|---|---|---|
| Sample: | 75BEA65B (batch 2 of 040218) smpl.1 | | | | | Chemisorption capacity: | 0.2530 | mmol/g at 170 Torr | | |
| Cat.mass: | 0.193 | g | | | Catalyst dry weigth: m_dry= | 0.17739 | g | | | |
| Cat.LOI: | 8.09 | % | | | Volume at temperature T1: V1= | 18.2623 | cc | | | |
| V_RMF: | 10.956 | cc | | | Volume at temperature T2: V2= | 0.93222 | cc | | | |
| Universal gas constant: R= | 62.3601 | cc*Torr/mmol/K | | | | 19.1945 | | | | |

**(A) Room temp. expansion in He**

| T1=T2= | 28 | | | R_0 |
|---|---|---|---|---|
| Pzero | Pinitial | Pfinal | Pzero_f | 0.57079 |
| 0.22 | 201.25 | 114.96 | 0.22 | 0.57076 |
| 0.22 | 200.91 | 114.77 | 0.22 | 0.57078 |
| 0.22 | 201.1 | 114.89 | 0.22 | 0.57084 |
| 0.22 | 201.65 | 115.19 | 0.22 | 0.57077 |

**(B) Expansion in He at ads. Temp**

| RMF_T1= | 27.8 | RXTR_T2= | 80 | R_T |
|---|---|---|---|---|
| Pzero | Pinitial | Pfinal | Pzero_f | 0.57491 |
| 0.2 | 201.71 | 117.59 | 0.2 | 0.58255 |
| 0.2 | 201.41 | 117.4 | 0.2 | 0.58248 |
| 0.21 | 201.39 | 117.36 | 0.21 | 0.58231 |
| 0.21 | 199.1 | 110.06 | 0.21 | 0.55232 |

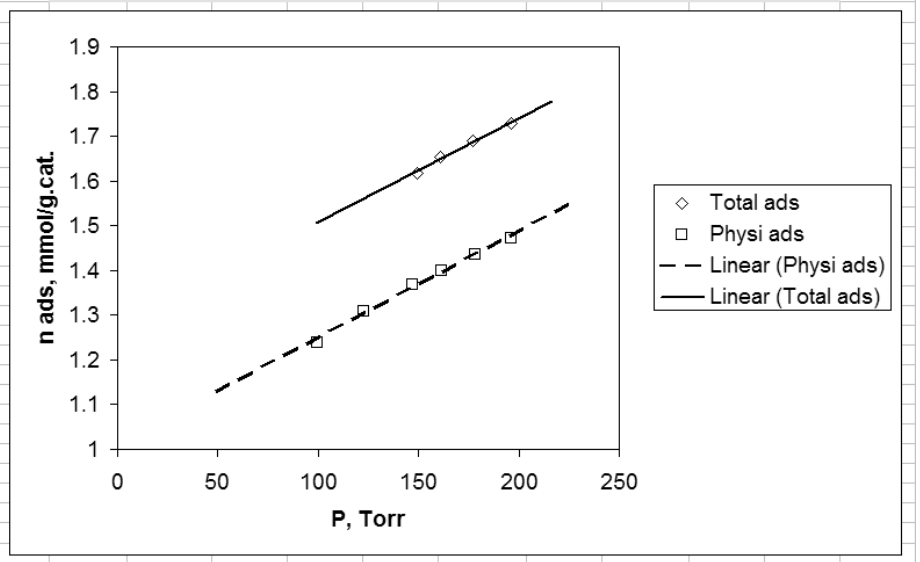


http://catalysis.che.wsu.edu/lab/equipment/RXM-100/INFP_Meter/acquire

**(C) Total adsorption at ads. Temp**

RXTR_T2= 80 P_zero= 0.19 P_calc= 170

| PoRMF meas | P meas | T1 | PoRMF | P | noRMF, mmol | n1, mmol | n2, mmol | nRMF, mmol | Δn_ads | n_ads, mmol/g |
|---|---|---|---|---|---|---|---|---|---|---|
| - | - | 27.7 | - | 0 | - | 0 | 0 | 0 | - | 0 |
| 750.91 | 149.29 | 27.5 | 750.72 | **149.1** | 0.438402 | 0.14523308 | 0.006311 | 0.0871287 | 0.28686 | **1.617137** |
| 180.5 | 161.05 | 27.6 | 180.31 | **160.86** | 0.105367 | 0.15663598 | 0.006809 | 0.0939696 | 0.00634 | **1.652863** |
| 201.01 | 177.5 | 27.7 | 200.82 | **177.31** | 0.117313 | 0.17259663 | 0.007506 | 0.1035448 | 0.00669 | **1.6905573** |
| 222.03 | 196.44 | 27.7 | 221.84 | **196.25** | 0.129549 | 0.19103316 | 0.008307 | 0.1146053 | 0.00677 | **1.7287011** |

R_squared= 0.9923879

**Total ads.at 170 Torr, mmol/g= 1.6702577**

**(D) Physical adsorption at ads. Temp**

RXTR_T2= 80 P_zero= 0.25

| PoRMF meas | P meas | T1 | PoRMF | P | noRMF, mmol | n1, mmol | n2, mmol | nRMF, mmol | Δn_ads | n_ads, mmol/g |
|---|---|---|---|---|---|---|---|---|---|---|
| - | - | 27.3 | - | 0 | - | 0 | 0 | 0 | - | 0 |
| 549.58 | 100 | 27.8 | 549.33 | **99.75** | 0.32122263 | 0.097066 | 0.00422245 | 0.058232 | 0.219934 | **1.239859** |
| 161.59 | 123.19 | 27.8 | 161.34 | **122.94** | 0.09418738 | 0.119632 | 0.00520409 | 0.07177 | 0.012407 | **1.309805** |
| 182.9 | 147.31 | 28 | 182.65 | **147.06** | 0.10662778 | 0.143008 | 0.00622509 | 0.085794 | 0.010461 | **1.368776** |
| 181.67 | 161.47 | 27.9 | 181.42 | **161.22** | 0.10583939 | 0.15683 | 0.00682449 | 0.094086 | 0.005624 | **1.400481** |
| 201.53 | 178.31 | 28.1 | 201.28 | **178.06** | 0.1174646 | 0.173097 | 0.00753733 | 0.103845 | 0.006399 | **1.436557** |
| 221.35 | 196.64 | 28.1 | 221.1 | **196.39** | 0.12894565 | 0.190916 | 0.00831325 | 0.114535 | 0.006506 | **1.473234** |

R_squared= 0.993892

**Physi ads.at 170 Torr, mmol/g= 1.417222**

**Chemi ads.at 170 Torr, mmol/g= 0.253035**

Table C1. Complete ammonia chemisorption data

| | NH3 chemisorption, mmol/g | | | | |
|---|---|---|---|---|---|
| material | run#1 | run#2 | run#3 | average | ±% |
| 25BEA65 | 0.576 | 0.564 | 0.575 | 0.572 | 1.3 |
| 75BEA65 | 0.253 | 0.237 | 0.271 | 0.254 | 7.5 |
| 80ZSM565 | 0.342 | 0.317 | 0.348 | 0.336 | 5.5 |
| SZ | 0.228 | 0.228 | 0.234 | 0.230 | 1.7 |
| 25BEA65B* | 0.567 | 0.688 | 0.457 | 0.570 | 22.9 |

* Samples of 25BEA65 that were activated in a stream of 20% oxygen diluted in ultra pure helium prior to being analyzed by ammonia chemisorption.

Table C2. Complete isobutane adsorption capacity data

| | iC4 total ads mmol/g | | | | |
|---|---|---|---|---|---|
| material | run1 | run2 | run3 | avg | ± % |
| 75BEA65 | 0.736 | 0.730 | - | 0.733 | 0.82 |
| 25BEA65 | 0.780 | 0.780 | - | 0.780 | 0.01 |
| SZ | 0.037 | 0.034 | 0.031 | 0.034 | 9.98 |
| 80ZSM565 | 0.377 | 0.383 | 0.371 | 0.377 | 1.80 |

## APPENDIX D

## RAW HYDRIDE TRANSFER TEST DATA

| | | | | % | % | % | % |
|---|---|---|---|---|---|---|---|
| catalyst= | 75BEA65 | #1 | | | | | |
| m cat= | 0.343 | g | TOS, min | MCP | MCPE-1 | CHX | CHXE |
| LOI= | 8.09 | % | 1 | 0 | 0 | 0 | 0.002592 |
| NH3 chemis= | 0.254 | mmol/g_dry | 4.2 | 0 | 0 | 0 | 0.001893 |
| iBU /rxtr= | 20.02 | sccm | 7.4 | 0.000197 | 0 | 0.002822 | 0.001997 |
| He /rxtr= | 20.02 | sccm | 10.6 | 0.000808 | 0 | 0.010542 | 0.00169 |
| He /sat= | 9.91 | sccm | 13.8 | 0.001107 | 0 | 0.018273 | 0.001795 |
| CHXE sat%= | 3.61 | % | 17 | 0.001048 | 0 | 0.02213 | 0.004611 |
| | | | 20.2 | 0.000969 | 0 | 0.024029 | 0.077948 |
| | | | 23.4 | 0.000437 | 0.000524 | 0.012712 | 0.402608 |
| | | | 26.6 | 0 | 0.00082 | 0.004447 | 0.715106 |
| | | | 29.8 | 0 | 0.000747 | 0.000843 | 0.726821 |
| | | | 33 | 0 | 0.000703 | 0.0003 | 0.749446 |
| | | | 36.2 | 0 | 0.000708 | 0 | 0.726631 |
| | | | 39.4 | 0 | 0.00056 | 0 | 0.691173 |
| | | | 42.6 | 0 | 0.000464 | 0 | 0.706485 |
| | | | 45.8 | 0 | 0.000449 | 0 | 0.605552 |

| | | | | % | % | % | % |
|---|---|---|---|---|---|---|---|
| catalyst= | 75BEA65 | #3 | | | | | |
| m cat= | 0.343 | g | TOS, min | MCP | MCPE-1 | CHX | CHXE |
| LOI= | 8.09 | % | 1 | 0 | 0 | 0 | 0.001133 |
| NH3 chemis= | 0.254 | mmol/g_dry | 4.2 | 0 | 0 | 0 | 0.000998 |
| iBU /rxtr= | 20.02 | sccm | 7.4 | 9.53E-05 | 0 | 0.002115 | 0.001054 |
| He /rxtr= | 20.02 | sccm | 10.6 | 0.000678 | 0 | 0.007929 | 0.000722 |
| He /sat= | 9.91 | sccm | 13.8 | 0.001055 | 0 | 0.016069 | 0.000663 |
| CHXE sat%= | 3.61 | % | 17 | 0.001071 | 0 | 0.020616 | 0.001231 |
| | | | 20.2 | 0.000709 | 0 | 0.016631 | 0.015961 |
| | | | 23.4 | 0.000571 | 7.79E-05 | 0.014335 | 0.143001 |
| | | | 26.6 | 0.000172 | 0.000425 | 0.008435 | 0.343596 |
| | | | 29.8 | 0 | 0.000714 | 0.001648 | 0.560838 |
| | | | 33 | 0 | 0.000818 | 0.000657 | 0.6599 |
| | | | 36.2 | 0 | 0.000768 | 0.000116 | 0.657241 |
| | | | 39.4 | 0 | 0.000678 | 0 | 0.630229 |
| | | | 42.6 | 0 | 0.000646 | 0 | 0.633428 |
| | | | 45.8 | 0 | 0.00068 | 3.45E-05 | 0.693977 |
| | | | 49 | 0 | 0.000578 | 0 | 0.687515 |

| | | | | % | % | % | % |
|---|---|---|---|---|---|---|---|
| catalyst= | 75BEA65 | #4 | | | | | |
| m cat= | 0.343 | g | TOS, min | MCP | MCPE-1 | CHX | CHXE |
| LOI= | 8.09 | % | 1 | 0 | 0 | 0 | 0.00113 |
| NH3 chemis= | 0.254 | mmol/g_dry | 4.2 | 0 | 0 | 0.000273 | 0.001159 |
| iBU /rxtr= | 20.02 | sccm | 7.4 | 0.000176 | 0 | 0.004597 | 0.000971 |
| He /rxtr= | 20.02 | sccm | 10.6 | 0.000665 | 0 | 0.011029 | 0.001532 |
| He /sat= | 9.91 | sccm | 13.8 | 0.000734 | 0 | 0.014409 | 0.024099 |
| CHXE sat%= | 3.61 | % | 17 | 0.000695 | 0 | 0.015157 | 0.116009 |
| | | | 20.2 | 0.000442 | 8.03E-05 | 0.01248 | 0.213585 |
| | | | 23.4 | 0.000343 | 0.000287 | 0.010468 | 0.327543 |
| | | | 26.6 | 5.98E-05 | 0.000351 | 0.007553 | 0.423862 |
| | | | 29.8 | 3.41E-05 | 0.000507 | 0.006197 | 0.574318 |
| | | | 33 | 0 | 0.000504 | 0.003006 | 0.614967 |
| | | | 36.2 | 0 | 0.000542 | 0.001365 | 0.680588 |
| | | | 39.4 | 0 | 0.000627 | 0.000816 | 0.788805 |
| | | | 42.6 | 0 | 0.000669 | 0.000238 | 0.79623 |
| | | | 45.8 | 0 | 0.00065 | 8.08E-05 | 0.741865 |

| | | | | % | % | % | % |
|---|---|---|---|---|---|---|---|
| catalyst= | 75BEA65 | #5 | | | | | |
| m cat= | 0.343 | g | TOS, min | MCP | MCPE-1 | CHX | CHXE |
| LOI= | 8.09 | % | 1 | 0 | 0 | 0 | 0.001417 |
| NH3 chemis= | 0.254 | mmol/g_dry | 4.2 | 0 | 0 | 0.000602 | 0.001326 |
| iBU /rxtr= | 20.02 | sccm | 7.4 | 0.000291 | 0 | 0.005164 | 0.00102 |
| He /rxtr= | 20.02 | sccm | 10.6 | 0.00073 | 0 | 0.011461 | 0.001527 |
| He /sat= | 9.91 | sccm | 13.8 | 0.000824 | 0 | 0.015373 | 0.018713 |
| CHXE sat%= | 3.61 | % | 17 | 0.000688 | 0 | 0.014228 | 0.07352 |
| acid sites= | 0.080074 | mmol | 20.2 | 0.00059 | 5.16E-05 | 0.013965 | 0.164575 |
| F_CHXE= | 0.016559 | mmol/min | 23.4 | 0.000487 | 0.000318 | 0.01241 | 0.276518 |
| CHXE_feed%= | 0.732162 | % | 26.6 | 0.000241 | 0.000354 | 0.008639 | 0.382195 |
| F_feed= | 2.245077 | mmol/min | 29.8 | 2.5E-05 | 0.000462 | 0.006206 | 0.467322 |
| iBU/CHXE= | 53.94053 | | 33 | 0 | 0.000478 | 0.003484 | 0.53942 |
| CHXE mol.S.V.= | 0.206794 | mmol/mmol_min | 36.2 | 0 | 0.0006 | 0.001691 | 0.583841 |
| | | | 39.4 | 0 | 0.000558 | 0.000658 | 0.639866 |
| | | | 42.6 | 0 | 0.000566 | 3.09E-05 | 0.662386 |
| | | | 45.8 | 0 | 0.00055 | 0 | 0.672974 |
| | | | 49 | 0 | 0.000559 | 0 | 0.657095 |

| | | | | | | | |
|---|---|---|---|---|---|---|---|
| catalyst= | 75BEA65 | #6 NIBU | | % | % | % | % |
| m cat= | 0.343 | g | TOS, min | MCP | MCPE-1 | CHX | CHXE |
| LOI= | 8.09 | % | 1 | 0 | 0 | 0 | 0.006767835 |
| NH3 chemis= | 0.254 | mmol/g_dry | 4.2 | 0 | 0 | 0 | 0.004254623 |
| iBU /rxtr= | 0 | sccm | 7.4 | 0 | 0 | 0 | 0.003061524 |
| He /rxtr= | 40.08 | sccm | 10.6 | 0 | 0 | 0 | 0.002216152 |
| He /sat= | 9.91 | sccm | 13.8 | 0 | 0 | 0 | 0.001672698 |
| CHXE sat%= | 3.61 | % | 17 | 0 | 0 | 0 | 0.001020971 |
| acid sites= | 0.08007383 | mmol | 20.2 | 0 | 0 | 0 | 0.00052749 |
| F_CHXE= | 0.016558825 | mmol/min | 23.4 | 0 | 0 | 0.001316486 | 0.023558673 |
| CHXE_feed%= | 0.731584226 | % | 26.6 | 0 | 0 | 0.001691261 | 0.074236576 |
| F_feed= | 2.246861314 | mmol/min | 29.8 | 0.000151923 | 0.000110559 | 0.004711734 | 0.221952503 |
| iBU/CHXE= | 0 | | 33 | 0.000457314 | 0.000260857 | 0.008050989 | 0.386961771 |
| CHXE mol.S.V.= | 0.206794463 | | 36.2 | 5.92242E-05 | 0.000503616 | 0.003407974 | 0.557109903 |
| (mmol/mmol_min) | | | 39.4 | 0 | 0.000537059 | 0.002560435 | 0.566057104 |
| | | | 42.6 | 0 | 0.000603158 | 0.000589842 | 0.621517814 |
| | | | 45.8 | 0 | 0.000557125 | 0.00015271 | 0.598361699 |
| | | | 49 | 0 | 0.000550436 | 0 | 0.609016996 |

| catalyst= | 25BEA65 | #4 | | % | % | % | % |
|---|---|---|---|---|---|---|---|
| m cat= | 0.155 | g | TOS, min | MCP | MCPE-1 | CHX | CHXE |
| LOI= | 9.55 | % | 1 | 0 | 0 | 0 | 0 |
| NH3 chemis= | 0.572 | mmol/g_dry | 4.2 | 0.001148597 | 0 | 0.023235124 | 0.002922931 |
| iBU /rxtr= | 20.02 | sccm | 7.4 | 0.001319369 | 0 | 0.041644737 | 0.049630165 |
| He /rxtr= | 20.02 | sccm | 10.6 | 0.000800097 | 0.000128535 | 0.030234653 | 0.253300264 |
| He /sat= | 9.91 | sccm | 13.8 | 0 | 0.000291861 | 0.011058428 | 0.537723908 |
| CHXE sat%= | 3.61 | % | 17 | 0 | 0.000429577 | 0.003121148 | 0.672230749 |
| | | | 20.2 | 0 | 0.000356129 | 0.000865075 | 0.721513129 |
| | | | 23.4 | 0 | 0.000330035 | 0 | 0.685482395 |
| | | | 26.6 | 0 | 0.000283647 | 0 | 0.751688624 |
| | | | 29.8 | 0 | 0.000283164 | 0 | 0.787742373 |
| | | | 33 | 0 | 0.000178789 | 0 | 0.725297 |
| | | | 36.2 | 0 | 0.000281714 | 0 | 0.760384963 |
| | | | 39.4 | 0 | 0.000253204 | 0 | 0.82791073 |
| | | | 42.6 | 0 | 0.000156561 | 0 | 0.759515499 |
| | | | 45.8 | 0 | 0.000200051 | 0 | 0.718276509 |

| catalyst= | 25BEA65 | #5 | | % | % | % | % |
|---|---|---|---|---|---|---|---|
| m cat= | 0.155 | g | TOS, min | MCP | MCPE-1 | CHX | CHXE |
| LOI= | 9.55 | % | 1.5 | 0 | 0 | 0.000967953 | 0.001356229 |
| NH3 chemis= | 0.572 | mmol/g_dry | 4.7 | 0.001226978 | 0 | 0.029467677 | 0.004329155 |
| iBU /rxtr= | 20.02 | sccm | 7.9 | 0.001043339 | 0 | 0.038576317 | 0.086861521 |
| He /rxtr= | 20.02 | sccm | 11.1 | 0.000624226 | 0 | 0.023685575 | 0.344140838 |
| He /sat= | 9.91 | sccm | 14.3 | 0 | 0.000196871 | 0.009559681 | 0.564685213 |
| CHXE sat%= | 3.61 | % | 17.5 | 0 | 0.000144825 | 0.0033979 | 0.65436298 |
| | | | 20.7 | 0 | 0.000274375 | 0.001404355 | 0.759456249 |
| | | | 23.9 | 0 | 0.000198568 | 4.66594E-05 | 0.714129862 |
| | | | 27.1 | 0 | 0.00010183 | 0 | 0.701795065 |
| | | | 30.3 | 0 | 0.000134642 | 0 | 0.691513073 |
| | | | 33.5 | 0 | 0.000268152 | 0 | 0.775752951 |
| | | | 36.7 | 0 | 6.67551E-05 | 0 | 0.652646487 |
| | | | 39.9 | 0 | 0.00016519 | 0 | 0.772917744 |
| | | | 43.1 | 0 | 0.000171413 | 0 | 0.686910478 |
| | | | 46.3 | 0 | 0.000188951 | 0 | 0.712144918 |

| catalyst= | 25BEA65 | #6 | | % | % | % | % |
|---|---|---|---|---|---|---|---|
| m cat= | 0.155 | g | TOS, min | MCP | MCPE-1 | CHX | CHXE |
| LOI= | 9.55 | % | 2 | 0 | 0 | 0.00257675 | 0.007764151 |
| NH3 chemis= | 0.572 | mmol/g_dry | 5.2 | 0.001228978 | 0 | 0.029630119 | 0.012414611 |
| iBU /rxtr= | 20.02 | sccm | 8.4 | 0.00119309 | 0.000231757 | 0.039476987 | 0.095010471 |
| He /rxtr= | 20.02 | sccm | 11.6 | 0.000618213 | 0.000533869 | 0.025738222 | 0.326759618 |
| He /sat= | 9.91 | sccm | 14.8 | 0 | 0.000623365 | 0.010358034 | 0.596958106 |
| CHXE sat%= | 3.61 | % | 18 | 0 | 0.00074959 | 0.003599921 | 0.774737824 |
| | | | 21.2 | 0 | 0.000677165 | 0.001084243 | 0.715909868 |
| | | | 24.4 | 0 | 0.000550941 | 0.000144733 | 0.751970099 |
| | | | 27.6 | 0 | 0.00048369 | 0 | 0.725844113 |
| | | | 30.8 | 0 | 0.000363672 | 0 | 0.689507374 |
| | | | 34 | 0 | 0.000405058 | 0 | 0.781359437 |
| | | | 37.2 | 0 | 0.000374536 | 0 | 0.702954102 |
| | | | 40.4 | 0 | 0.000266417 | 0 | 0.781275481 |
| | | | 43.6 | 0 | 0.0002659 | 0 | 0.708862998 |
| | | | 46.8 | 0 | 0.000259692 | 0 | 0.719785556 |

| catalyst= | 25BEA65 | #7 | | % | % | % | % |
|---|---|---|---|---|---|---|---|
| m cat= | 0.155 | g | TOS, min | MCP | MCPE-1 | CHX | CHXE |
| LOI= | 9.55 | % | 3 | 0.000323665 | 0 | 0.007341843 | 0.000596311 |
| NH3 chemis= | 0.572 | mmol/g_dry | 6.2 | 0.001341473 | 0 | 0.036987839 | 0.00452016 |
| iBU /rxtr= | 20.02 | sccm | 9.4 | 0.001037943 | 0 | 0.039812629 | 0.109736838 |
| He /rxtr= | 20.02 | sccm | 12.6 | 0.000281382 | 0.000121139 | 0.014722246 | 0.391344228 |
| He /sat= | 9.91 | sccm | 15.8 | 0 | 0.000245739 | 0.003605308 | 0.604990473 |
| CHXE sat%= | 3.61 | % | 19 | 0 | 0.00028881 | 0.001206538 | 0.752936672 |
| | | | 22.2 | 0 | 0.000237663 | 0.000334596 | 0.683629588 |
| | | | 25.4 | 0 | 0.000200744 | 0.000113191 | 0.696276945 |
| | | | 28.6 | 0 | 0.000170363 | 0 | 0.668571886 |
| | | | 31.8 | 0 | 0.000307269 | 0 | 0.807027309 |
| | | | 35 | 0 | 0.000309192 | 0 | 0.8068109 |
| | | | 38.2 | 0 | 0.00038649 | 0 | 0.686182396 |

| | | | | % | % | % | % |
|---|---|---|---|---|---|---|---|
| catalyst= | 25BEA65 | #8 no iBU | | | | | |
| m cat= | 0.155 | g | TOS, min | MCP | MCPE-1 | CHX | CHXE |
| LOI= | 9.55 | % | 1 | 0 | 0 | 0 | 0 |
| NH3 chemis= | 0.572 | mmol/g_dry | 4.2 | 0 | 0 | 0 | 0.000305036 |
| iBU /rxtr= | | sccm | 7.4 | 0 | 0 | 0.00058436 | 0.022301981 |
| He /rxtr= | 40.08 | sccm | 10.6 | 0 | 0 | 0.005794103 | 0.227662663 |
| He /sat= | 9.91 | sccm | 13.8 | 0.000236221 | 0.000261165 | 0.009080406 | 0.545312318 |
| CHXE sat%= | 3.61 | % | 17 | 0.000177426 | 0.000385587 | 0.007575469 | 0.6535089 |
| | | | 20.2 | 0 | 0.000376444 | 0.00292823 | 0.68767853 |
| | | | 23.4 | 0 | 0.000422953 | 0.002043011 | 0.711657156 |
| | | | 26.6 | 0 | 0.000319997 | 0.000196072 | 0.70945108 |
| | | | 29.8 | 0 | 0.000264346 | 0 | 0.723180501 |
| | | | 33 | 0 | 0.000299327 | 0 | 0.712158537 |
| | | | 36.2 | 0 | 0.000264743 | 0 | 0.704191841 |
| | | | 39.4 | 0 | 0.000243675 | 0 | 0.686503265 |
| | | | 42.6 | 0 | 0.000245662 | 0 | 0.666108635 |
| | | | 45.8 | 0 | 0.000203924 | 0 | 0.68568072 |

| catalyst= | SZ | #1 | | % | % | % | % |
|---|---|---|---|---|---|---|---|
| m cat= | 0.356 | g | TOS, min | MCP | MCPE-1 | CHX | CHXE |
| LOI= | 2.56 | % | 1 | 0.003561341 | 0 | 0.005424738 | 0 |
| NH3 chemis= | 0.23 | mmol/g_dry | 4.2 | 0.009057099 | 0 | 0.022669265 | 0.159658118 |
| iBU /rxtr= | 20.02 | sccm | 7.4 | 0.002867072 | 4.50197E-05 | 0.00852232 | 0.395624588 |
| He /rxtr= | 20.02 | sccm | 10.6 | 0.000302671 | 0.000198905 | 0.002016737 | 0.515467989 |
| He /sat= | 9.91 | sccm | 13.8 | 0 | 0.000160025 | 0.000611574 | 0.531018594 |
| CHXE sat%= | 3.61 | % | 17 | 0 | 0.000220187 | 0.000342852 | 0.600878271 |

| catalyst= | SZ | #2 | | % | % | % | % |
|---|---|---|---|---|---|---|---|
| m cat= | 0.357 | g | TOS, min | MCP | MCPE-1 | CHX | CHXE |
| LOI= | 2.56 | % | 1 | 0.012059614 | 9.80631E-05 | 0.022533271 | 0.030941079 |
| NH3 chemis= | 0.23 | mmol/g_dry | 4.2 | 0.007755244 | 0.000445793 | 0.018833779 | 0.404903421 |
| iBU /rxtr= | 20.02 | sccm | 7.4 | 0.003832254 | 0.000486371 | 0.010380271 | 0.48040892 |
| He /rxtr= | 20.02 | sccm | 10.6 | 0.001369874 | 0.000463264 | 0.004764953 | 0.582793252 |
| He /sat= | 9.91 | sccm | 13.8 | 0.000258188 | 0.000490879 | 0.001623256 | 0.618358294 |
| CHXE sat%= | 3.61 | % | 17 | 0 | 0.000490316 | 0.000420169 | 0.703315526 |
| | | | 20.2 | 0 | 0.000444666 | 0 | 0.642847101 |
| | | | 23.4 | 0 | 0.000482989 | 5.10401E-05 | 0.732329871 |
| | | | 26.6 | 0 | 0.000450301 | 0 | 0.735352199 |
| | | | 29.8 | 0 | 0.000485807 | 0 | 0.722682283 |

| catalyst= | SZ | #3 | | % | % | % | % |
|---|---|---|---|---|---|---|---|
| m cat= | 0.357 | g | TOS, min | MCP | MCPE-1 | CHX | CHXE |
| LOI= | 2.56 | % | 0.5 | 0 | 0 | 0 | 0 |
| NH3 chemis= | 0.23 | mmol/g_dry | 3.7 | 0.010642258 | 0 | 0.026518142 | 0.031423799 |
| iBU /rxtr= | 20.02 | sccm | 6.9 | 0.000350747 | 0 | 0.002991931 | 0.457909736 |
| He /rxtr= | 20.02 | sccm | 10.1 | 0 | 5.91483E-05 | 0.000646297 | 0.548177172 |
| He /sat= | 9.91 | sccm | 13.3 | 0 | 0.000146585 | 0.000212937 | 0.699538374 |
| CHXE sat%= | 3.61 | % | 16.5 | 0 | 0.000178988 | 0 | 0.685113041 |
| | | | 19.7 | 0 | 0.00020059 | 0 | 0.700806794 |
| | | | 22.9 | 0 | 0.000310657 | 0 | 0.681767786 |
| | | | 26.1 | 0 | 0.000326087 | 0 | 0.72962389 |
| | | | 29.3 | 0 | 0.000339974 | 0 | 0.644992669 |

| catalyst= | SZ | #4, No IBU | | % | % | % | % |
|---|---|---|---|---|---|---|---|
| m cat= | 0.357 | g | TOS, min | MCP | MCPE-1 | CHX | CHXE |
| LOI= | 2.56 | % | 0.5 | 0 | 0 | 0 | 0.007051673 |
| NH3 chemis= | 0.23 | mmol/g_dry | 3.7 | 0.01096386 | 0 | 0.001956135 | 0.005201336 |
| iBU /rxtr= | | sccm | 6.9 | 0.003354817 | 3.17853E-05 | 0.003795443 | 0.330692597 |
| He /rxtr= | 40.08 | sccm | 10.1 | 0 | 9.47779E-05 | 0.000200941 | 0.511402816 |
| He /sat= | 9.91 | sccm | 13.3 | 0 | 0.000517233 | 0.000101872 | 0.607025018 |
| CHXE sat%= | 3.61 | % | 16.5 | 0 | 0.000805612 | 0 | 0.65025462 |
| | | | 19.7 | 0 | 0.000664601 | 0 | 0.686957577 |
| | | | 22.9 | 0 | 0.001189346 | 0 | 0.684137723 |
| | | | 26.1 | 0 | 0.001139646 | 0 | 0.714170287 |

| catalyst= | 80ZSM565 | #1 | | % | % | % | % |
|---|---|---|---|---|---|---|---|
| m cat= | 0.2485 | g | TOS, min | MCP | MCPE-1 | CHX | CHXE |
| LOI= | 4.33 | % | 1 | 0 | 0 | 0 | 0 |
| NH3 chemis= | 0.336 | mmol/g_dry | 4.2 | 0.022367131 | 0.009359784 | 0 | 0.079485751 |
| iBU /rxtr= | 20.02 | sccm | 7.4 | 0.017367982 | 0.02856215 | 0 | 0.325911664 |
| He /rxtr= | 20.02 | sccm | 10.6 | 0.009992696 | 0.040070273 | 0 | 0.526171602 |
| He /sat= | 9.91 | sccm | 13.8 | 0.005677405 | 0.043720652 | 0 | 0.629875916 |
| CHXE sat%= | 3.61 | % | 17 | 0.003184366 | 0.040572475 | 0 | 0.647862404 |
| | | | 20.2 | 0.001947371 | 0.036804821 | 0 | 0.684680519 |
| | | | 23.4 | 0.000602438 | 0.030672824 | 0 | 0.637075948 |
| | | | 26.6 | 0.000703653 | 0.032541243 | 0 | 0.722503336 |
| | | | 29.8 | 0.000670413 | 0.030728181 | 0 | 0.75787933 |
| | | | 33 | 0 | 0.026640088 | 0 | 0.709065693 |
| | | | 36.2 | 0 | 0.028039975 | 0 | 0.791821257 |
| | | | 39.4 | 0 | 0.024461217 | 0 | 0.750683325 |
| | | | 42.6 | 0 | 0.023425426 | 0 | 0.741605265 |
| | | | 45.8 | 0 | 0.022195317 | 0 | 0.758578494 |
| | | | 49 | 0 | 0.020646482 | 0 | 0.728528026 |
| | | | 52.2 | 0 | 0.019285401 | 0 | 0.727396981 |
| | | | 55.4 | 0 | 0.019059981 | 0 | 0.751323596 |
| | | | 61.8 | 0 | 0.018554926 | 0 | 0.816612641 |

| catalyst= | 80ZSM565 | #2 | | % | % | % | % |
|---|---|---|---|---|---|---|---|
| m cat= | 0.249 | g | TOS, min | MCP | MCPE-1 | CHX | CHXE |
| LOI= | 4.33 | % | 1 | 0 | 0.001177725 | 0 | 0.002102034 |
| NH3 chemis= | 0.336 | mmol/g_dry | 4.2 | 0.017542971 | 0.010081949 | 0.000722198 | 0.113664926 |
| iBU /rxtr= | 20.02 | sccm | 7.4 | 0.014074676 | 0.029362971 | 0.001271248 | 0.436840369 |
| He /rxtr= | 20.02 | sccm | 10.6 | 0.006718028 | 0.03274692 | 0.001061766 | 0.562909544 |
| He /sat= | 9.91 | sccm | 13.8 | 0.0037729 | 0.032003283 | 0.000894449 | 0.614439706 |
| CHXE sat%= | 3.61 | % | 17 | 0.002602401 | 0.032657883 | 0.00076257 | 0.659501318 |
| | | | 23.4 | 0.001012569 | 0.025082275 | 0.000462027 | 0.655645144 |
| | | | 26.6 | 0.000867709 | 0.027517054 | 0.000510473 | 0.848404958 |
| | | | 29.8 | 0.000682186 | 0.023865163 | 0.000377696 | 0.714125814 |
| | | | 33 | 0.000640072 | 0.0237789 | 0.000383976 | 0.748678237 |
| | | | 36.2 | 0.000510823 | 0.021894428 | 0.000218005 | 0.744007867 |
| | | | 39.4 | 0.000438211 | 0.022378167 | 0.000183465 | 0.745244328 |

| | | | | % | % | % | % |
|---|---|---|---|---|---|---|---|
| catalyst= | 80ZSM565 | #3 | | | | | |
| m cat= | 0.249 | g | TOS, min | MCP | MCPE-1 | CHX | CHXE |
| LOI= | 4.33 | % | 1 | 0 | 0 | 0 | 0.0011749 |
| NH3 chemis= | 0.336 | mmol/g_dry | 4.2 | 0.022961168 | 0.011645941 | 0.001074366 | 0.102671926 |
| iBU /rxtr= | 20.02 | sccm | 7.4 | 0.022375268 | 0.03483099 | 0.001818494 | 0.386414394 |
| He /rxtr= | 20.02 | sccm | 10.6 | 0.010370516 | 0.038800759 | 0.001410618 | 0.486061997 |
| He /sat= | 9.91 | sccm | 13.8 | 0.006428525 | 0.044225299 | 0.001334073 | 0.62819147 |
| CHXE sat%= | 3.61 | % | 17 | 0.003274224 | 0.037168157 | 0.000805911 | 0.621456969 |
| | | | 20.2 | 0.002195797 | 0.035850648 | 0.000788962 | 0.664915139 |
| | | | 23.4 | 0.001354562 | 0.032523236 | 0.000581196 | 0.660390284 |
| | | | 26.6 | 0.001135955 | 0.030726664 | 0.000541284 | 0.68862903 |
| | | | 29.8 | 0.000798311 | 0.029234366 | 0.00032641 | 0.704964908 |
| | | | 33 | 0.000637675 | 0.027759986 | 0.000347734 | 0.712712089 |
| | | | 36.2 | 0.000468189 | 0.026504346 | 0.000356482 | 0.712854032 |
| | | | 39.4 | 0.000478367 | 0.025247354 | 0.000215967 | 0.74272392 |
| | | | 42.6 | 0.000386322 | 0.023653631 | 8.52932E-05 | 0.680863956 |

| | | | | % | % | % | % |
|---|---|---|---|---|---|---|---|
| catalyst= | 80ZSM565 | #4 no iBU | | | | | |
| m cat= | 0.249 | g | TOS, min | MCP | MCPE-1 | CHX | CHXE |
| LOI= | 4.33 | % | 1 | 0 | 0 | 0 | 0.002606285 |
| NH3 chemis= | 0.336 | mmol/g_dry | 4.2 | 0 | 0 | 0 | 0.001856757 |
| iBU /rxtr= | 0 | sccm | 7.4 | 0 | 0.010324133 | 0 | 0.088369335 |
| He /rxtr= | 40.08 | sccm | 10.6 | 0 | 0.032326866 | 5.8658E-05 | 0.426658681 |
| He /sat= | 9.91 | sccm | 13.8 | 0.006877669 | 0.035742566 | 0.000125137 | 0.569555254 |
| CHXE sat%= | 3.61 | % | 17 | 0.017780386 | 0.032409771 | 3.24015E-05 | 0.609037092 |
| | | | 20.2 | 0.014851804 | 0.030838024 | 6.20099E-05 | 0.66300066 |
| | | | 23.4 | 0.010054029 | 0.024166562 | 0 | 0.59604101 |
| | | | 26.6 | 0.007508872 | 0.023968971 | 0 | 0.644940086 |
| | | | 29.8 | 0.004717291 | 0.024452931 | 3.0167E-05 | 0.730420387 |
| | | | 33 | 0.003662423 | 0.020532544 | 0 | 0.671247904 |
| | | | 36.2 | 0.003056089 | 0.020337717 | 0 | 0.703843835 |
| | | | 39.4 | 0.001926615 | 0.019020213 | 0 | 0.701069363 |
| | | | 42.6 | 0.001615988 | 0.017376614 | 0 | 0.673806049 |
| | | | 45.8 | 0.001324802 | 0.016364824 | 0 | 0.668500245 |
| | | | 49 | 0.001001514 | 0.016319571 | 0 | 0.698533156 |

## APPENDIX E

## RAW ALKYLATION TEST DATA

Reactor feed calculation:

| | Ar% | Bue% | Bue/Ar | Ar/TMP | I/O | |
|---|---|---|---|---|---|---|
| test 1 | 16.0 | 3.4 | 0.913 | 1.9 | 23.9 | |
| | 14.5 | 3.2 | 0.956 | 1.7 | 25.9 | |
| | 13.3 | 3.1 | 1.021 | 1.6 | 26.7 | |
| | 13.1 | 3.4 | 1.136 | 1.6 | 24.4 | |
| test 2 | 26.5 | 4.9 | 0.810 | 3.2 | 13.9 | |
| | 25.0 | 5.0 | 0.866 | 3.0 | 14.0 | |
| | 22.4 | 4.8 | 0.921 | 2.7 | 15.3 | |
| test 3 | 16.9 | 4.2 | 1.084 | 2.0 | 18.7 | |
| | 15.3 | 4.1 | 1.173 | 1.9 | 19.5 | |
| | 14.0 | 4.1 | 1.284 | 1.7 | 19.8 | |
| | 17.70 | 4.02 | 1.02 | 2.14 | 20.2 | =avg |
| | 18.01 | 7.72 | | | | =theoretical (HYSYS) |

| | | | | |
|---|---|---|---|---|
| p, psig= | 47 | ==> n, mmol= | | 14.5 |
| V, cc= | 100 | nBUE1 feed, mmol= | | 0.583 |
| T, C= | 80 | n acid= | | 0.093 |
| R, l*atm/mol/k= | 0.082 | BUE1/acid= | | 6.27 |

| cat. Acid mmol= | | 0.093 | Bue | C8= | TMP | DMH | Bue conv | nC5 |
|---|---|---|---|---|---|---|---|---|
| material | Reaction time, min | | % | % | % | % | % | % |
| 75BEA652 | | 30.00 | 0.9332 | 0.0591 | 0.0123 | 0.0057 | 76.81 | 0.0149 |
| | | 60.00 | 0.6191 | 0.0551 | 0.0108 | 0.0062 | 84.62 | 0.0129 |
| | | 90.00 | 0.5119 | 0.0546 | 0.0101 | 0.0069 | 87.28 | 0.0157 |
| | | 120.00 | 0.4691 | 0.0591 | 0.0115 | 0.0069 | 88.34 | 0.0158 |
| | | 150.00 | 0.4254 | 0.0669 | 0.0122 | 0.0096 | 89.43 | 0.0144 |
| | | 180.00 | 0.3820 | 0.0706 | 0.0129 | 0.0083 | 90.51 | 0.0201 |
| | | 210.00 | 0.3788 | 0.0697 | 0.0136 | 0.0100 | 90.59 | 0.0220 |
| | | 10.00 | 0.8727 | 0.0535 | 0.0129 | 0.0056 | 78.32 | 0.0172 |
| | | 40.00 | 0.5230 | 0.0584 | 0.0136 | 0.0071 | 87.01 | 0.0188 |
| | | 70.00 | 0.4173 | 0.0610 | 0.0148 | 0.0079 | 89.63 | 0.0215 |
| | | 100.00 | 0.3638 | 0.0698 | 0.0166 | 0.0096 | 90.96 | 0.0234 |
| | | 130.00 | 0.3398 | 0.0709 | 0.0168 | 0.0101 | 91.56 | 0.0238 |
| | | 5.00 | 1.3392 | 0.0377 | 0.0104 | 0.0032 | 66.73 | 0.0110 |
| | | 35.00 | 0.9227 | 0.0465 | 0.0103 | 0.0045 | 77.07 | 0.0148 |
| | | 65.00 | 0.8115 | 0.0467 | 0.0106 | 0.0053 | 79.84 | 0.0168 |
| | | 95.00 | 0.6619 | 0.0500 | 0.0107 | 0.0051 | 83.55 | 0.0158 |
| | | 125.00 | 0.6029 | 0.0512 | 0.0107 | 0.0056 | 85.02 | 0.0176 |
| | | 155.00 | 0.5953 | 0.0521 | 0.0110 | 0.0056 | 85.21 | 0.0150 |
| 25BEA65 | | | 1.9106 | 0.0584 | 0.0283 | 0.0044 | 52.53 | 0.0264 |
| | | 35.00 | 1.7501 | 0.0637 | 0.0262 | 0.0056 | 56.52 | 0.0253 |
| | | 65.00 | 1.7381 | 0.0664 | 0.0264 | 0.0054 | 56.82 | 0.0258 |
| | | 95.00 | 1.6733 | 0.0680 | 0.0264 | 0.0060 | 58.43 | 0.0270 |
| | | 125.00 | 1.6781 | 0.0754 | 0.0270 | 0.0070 | 58.31 | 0.0319 |
| | | 10.00 | 1.6762 | 0.0520 | 0.0229 | 0.0041 | 58.36 | 0.0218 |
| | | 40.00 | 1.6717 | 0.0581 | 0.0237 | 0.0043 | 58.47 | 0.0234 |
| | | 70.00 | 1.6820 | 0.0603 | 0.0236 | 0.0051 | 58.21 | 0.0219 |
| | | 100.00 | 1.6679 | 0.0606 | 0.0241 | 0.0051 | 58.56 | 0.0245 |
| | | 130.00 | 1.5981 | 0.0612 | 0.0242 | 0.0055 | 60.29 | 0.0244 |

| cat. Acid mmol= | | 0.093 | Bue | C8= | TMP | DMH | Bue conv | nC5 |
|---|---|---|---|---|---|---|---|---|
| material | Reaction time, min | | % | % | % | % | % | % |
| SZ | | 10.00 | 2.5186 | 0.0501 | 0.0137 | 0.0061 | 37.43 | 0.0753 |
| | | 40.00 | 2.7955 | 0.0579 | 0.0126 | 0.0067 | 30.54 | 0.0808 |
| | | 70.00 | 2.8497 | 0.0648 | 0.0127 | 0.0070 | 29.20 | 0.0754 |
| | | 100.00 | 2.8343 | 0.0760 | 0.0134 | 0.0078 | 29.58 | 0.0758 |
| | | 130.00 | 2.6565 | 0.0827 | 0.0148 | 0.0093 | 34.00 | 0.0721 |
| | | 5.00 | 2.6148 | 0.0428 | 0.0116 | 0.0055 | 35.03 | 0.1215 |
| | | 35.00 | 3.0461 | 0.0626 | 0.0129 | 0.0076 | 24.32 | 0.1253 |
| | | 65.00 | 3.0709 | 0.0708 | 0.0143 | 0.0075 | 23.70 | 0.1220 |
| | | 95.00 | 3.0440 | 0.0796 | 0.0143 | 0.0093 | 24.37 | 0.1210 |
| | | 125.00 | 2.9304 | 0.0838 | 0.0143 | 0.0089 | 27.19 | 0.1169 |
| 25BEA65-HH | | 10.00 | 1.6888 | 0.0391 | 0.0147 | 0.0006 | 58.04 | 0.0159 |
| | | 40.00 | 1.8227 | 0.0534 | 0.0157 | 0.0017 | 54.71 | 0.0190 |
| | | 70.00 | 1.9426 | 0.0585 | 0.0178 | 0.0020 | 51.74 | 0.0193 |
| | | 100.00 | 1.9754 | 0.0643 | 0.0178 | 0.0035 | 50.92 | 0.0173 |
| | | 143.00 | 1.8569 | 0.0656 | 0.0178 | 0.0028 | 53.86 | 0.0195 |
| SZ-HH | | 10.00 | 1.9612 | 0.0380 | 0.0082 | 0.0012 | 51.27 | 0.0941 |
| | | 40.00 | 2.2212 | 0.0514 | 0.0075 | 0.0026 | 44.81 | 0.1021 |
| | | 70.00 | 2.4235 | 0.0629 | 0.0090 | 0.0034 | 39.79 | 0.1028 |
| | | 100.00 | 2.5572 | 0.0721 | 0.0091 | 0.0040 | 36.47 | 0.1039 |
| | | 130.00 | 2.5462 | 0.0755 | 0.0097 | 0.0056 | 36.74 | 0.1058 |
| | | 10.00 | 2.0068 | 0.0359 | 0.0087 | 0.0017 | 50.14 | 0.1230 |
| | | 40.00 | 2.2515 | 0.0487 | 0.0082 | 0.0024 | 44.06 | 0.1190 |
| | | 70.00 | 2.3257 | 0.0556 | 0.0089 | 0.0028 | 42.22 | 0.1207 |
| | | 100.00 | 2.4103 | 0.0591 | 0.0084 | 0.0027 | 40.12 | 0.1274 |
| | | 130.00 | 2.4706 | 0.0751 | 0.0099 | 0.0049 | 38.62 | 0.1216 |
| 80ZSM565 | | 10.00 | 1.3908 | 0.0000 | 0.0000 | 0.0000 | 65.44 | 0.0000 |
| | | 40.00 | 2.1530 | 0.0029 | 0.0000 | 0.0000 | 46.51 | 0.0000 |
| | | 70.00 | 2.2661 | 0.0025 | 0.0000 | 0.0000 | 43.70 | 0.0000 |